Supplemental Methods

Cell lines and primary samples

THP-1, KG-1 AML cell lines and TIME endothelial cell line have been obtained from the American Type Culture Collection (ATCC) while OCI-AML3 AML cell line been obtained from DSMZ. All the AML cell lines were maintained in culture with RPMI medium (EuroClone) supplemented with 10% heat-inactivated fetal bovine serum (FBS) (Gibco, Thermo Fisher Scientific), 2 mM L-glutamine, 25 IU/mL of penicillin and 25 mg/mL of streptomycin (Lonza). The MHH-CALL-4 cell line was maintained in culture in RPMI Advanced complete medium (Thermo Fisher Scientific) with 20% FBS. The TIME cell line was maintained in culture with Vascular Cell Basal Medium (ATCC), supplemented with the Microvascular Endothelial Cell Growth Kit-VEGF, containing several purified human recombinant (rh) growth factors (rh_VEGF [vascular endothelial growth factor], rh_EGF [epidermal growth factor], rh_FGF [fibroblast growth factor] basic, and rh IGF-1 [insulin growth factor 1]) and combined with 10 mM L-glutamine, 0.75 U/mL of heparin sulfate, 1 mg/mL of hydrocortisone hemisuccinate, 5% FBS, and 50 mg/mL of ascorbic acid (ATCC). 293T cell lines were maintained in DMEM High Glucose (Gibco) and 10% FBS.

OCI-AML3 (both wt and KO clones) and KG-1 cell lines were lentivirally transduced to express the green fluorescent protein and firefly luciferase (GFP-Luc). G-CSF-mobilized CD34+ cells were obtained from left-over samples of adult healthy donors, according to a University of Perugia IRB-approved informed consent form for clinical hematopoietic stem/progenitor cell donation. Apheresis products were labelled with CliniMACS CD34 MicroBeads (Miltenyi Biotec) and enriched with the CliniMACS Cell Separation System (Miltenyi Biotec). Primary AML cells were obtained from BM and PBMCs collected from AML patients. The Institutional Review Board of the Ethical Committee of San Gerardo Hospital approved this study, and informed consent was obtained from patients or their guardians.

Generation of CD33 and/or CD123 KO clones by CRISPR/CAS9 editing

CD33-KO, CD123-KO, and CD33/CD123 double-KO single cell clones were generated by CRISPR-mediated genome editing from the parental wt GFP-Luc OCI-AML3 and KG-1 cells, through electroporation (Neon transfector, ThermoFisher Scientific). Before electroporation, 1.5 µg of Cas9 protein (IDT- Integrated DNA Technologies) was incubated for at least 15-30 minutes with 1µg of sgRNA to form the RNP complex. Guide RNA sequences for CD33 and CD123 were respectively GGCCGGGTTCTAGAGTGCCA and GGCGTACTGGACGTCCGCGG, ordered from Synthego Biosciences. Off-targets and mismatches analysis for the corresponding gRNA, performed through

the Off-Spotter algorithm (https://cm.jefferson.edu/Off-Spotter/)[1], are shown in supplemental Fig.1 A and B respectively for CD123 sgRNA and CD33 sgRNA. Generally, 250,000 cells were electroporated according to optimized protocols for both OCI-AML3 and KG-1 cell lines (1400 V, 20 ms, 2 pulse). The isolation of knock-out clones for CD33 and/or CD123 gene was performed by a first enrichment through magnetic activated cell sorting (MACS). CD33 or anti-CD123 MicroBeads (MiltenyiBiotec) were used to enrich the edited population, further purified by cell sorting (FACSAria, BD Biosciences). Finally, single cloning allowed isolating a homogeneous monoclonal population either GFP-Luc CD33 KO, CD123KO or double CD33/CD123 KO.

Cell proliferation and competition assays

Proliferation assay was performed monitoring the luminescence emitted by GFP-Luc OCI-AML3 wt and KO clones 2-h after luciferine exposure. GFP-Luc OCI-AML3 cells were seeded in triplicates in 96-wells plates at a density of 250.000 per ml in 200 ml per well. Luminescence intensity was detected every 24 hours for 3 days through the automated Spark plate reader (Tecan), according to the manufacturer's protocol. In cell competition assays, OCI-AML3 wt and GFP-Luc KO clones were mixed and co-cultured from day 0 in a 6 well plate (1:1 ratio). An aliquot of the mixture was sampled, and new medium was refilled every 48 hours. Clonal evolution was estimated until day 9 by flow cytometry (FACS Canto II) using the ratio of the GFP− and GFP+ cell populations.

RNA sequencing

The total RNA from 12 samples (triplicates of OCI-AML3 wt, -CD33KO, -CD123KO and -CD33/123KO) was isolated according to RNeasy kit manufacturer's instructions (QIAGEN). The RNA quantity was assessed using NanoDrop 2000 spectrophotometer (Thermo Fisher Scientific) and Qubit 2.0 Flurometer (Life Technologies), while RNA Integrity Number (RIN) values were evaluated by microfluidic electrophoresis on a BioAnalyzer 2100 (Agilent Technologies). The RIN value score was ranging from 9 to 10. The 12 mRNA-libraries were prepared according to NEBNext Ultra II Directional's manufactures instruction kit with PolyA selection. Libraries preparation and sequencing were carried out at BIODIVERSA. Each sample was analyzed using our custom pipeline ARPIR[2] (https://github.com/giuliospinozzi/creo_pipelines) on HP Z840 workstation with 2x Intel Xeon and 256GB of RAM. Raw data are stored in a Network attached storage (NAS, QNAP TS-853A-4G-US with 32TB of space in RAID 6). ARPIR uses HISAT2 for the alignment, featureCounts for transcript quantification and edgeR for differential expression analysis.

After the quality check and the alignment (to hg19), Samtools was used to sort and index the bam files. After that, featureCounts was used to generate transcript abundance files. Once all samples

within each species were mapped and abundance count files were completed, edgeR filtered the genes to keep those that have at least one count per million in at least two samples. After filtering, the data were normalized through the TMM method (Trimmed Mean of M values). The model used is a Generalized Linear Model (GLM), which represents an extension of the simplest linear model. Each gene is fitted through a negative binomial distribution. Differential Expression Analysis is performed by a likelihood ratio test. Statistically significant DEGs (adjusted p-value<0.05 and absolute log Fold Change (logFC) > 1.5) were identified for each comparison using edgeR package.

Cloning of the anti-CD123.CAR, anti-CD33.CCR, retroviral supernatant production and CIK cells' transduction.

The retroviral supernatant was produced by Fugene (Promega) mediated co-transfection of 293T cells with the MoMLV gag-pol expression plasmid pEQPAM3(-E), the RD114 env expression plasmid pRDF and the SFG-2A-dual car vector.

Generation of CIK cells

PBMCs of healthy subjects were obtained after centrifugation of fresh blood on a density gradient using Ficoll-Hypaque (Pharmacia LKB). Cells were then resuspended in complete Advanced RPMI medium. At the beginning of the culture, gamma-interferon (IFN-gamma) (Domp_eBiotec S.p.A) was added at 1000 U/ml. The next day, IL2 (Chiron B.V) and OKT3 (Janssen-Cilag S.p.A.) were added at 300 U/ml and at 50 ng/ml, respectively, and cells were kept at the initial concentration of $3x10^6$ cells/ml. For viral transduction, CIK cells were genetically modified at day 5 as previously described[3]. For SB-transposon engineering CIK cells were transduced at day 0, as previously described[4]. Cells were then cultured for 21 days. Fresh medium and IL2 were added twice a week during culture and cell concentration was maintained around $0,75x10^6$ cells/ml.

Flow Cytometry

Immunostaining and flow cytometric analysis were performed on target cells and on CAR-CIK cells. Target cells were stained with: APC-anti-CD123 (Becton Dickinson, BD), PE-anti-CD123 (BD), FITC or PeCy7 anti-CD33 (BD), PeCy7 anti-CD34 (BD), PerCP- anti-CD38 (Invitrogen), PE-anti-CD144 (BD). BD QuantiBRITE PE fluorescence quantitation kit was used together with PE-anti-CD123 and PE-anti-CD33 (BD) to measure the number of molecules/cell. Mean number of CD33 and CD123 molecules on the cell surface was estimated by PE fluorescence intensity, as antibody binding capacity (ABC). QuantiBRITE beads labeled with different PE levels were used to generate the standard curve for fluorescent intensity versus the number of PE molecules/bead.

CIK cells were stained with PerCP-anti-CD3 (Biolegend, San Diego, CA, USA), PE-anti-CD56 (BD), FITC (BD) or APC-H7 (Biolegend) anti-CD8, PE (BD) or PB (Biolegend) anti-CD4, PE-anti-CD62L (BD), FITC-anti-CD45RO (BD), Alexa Fluor 647-F(ab0)2-antiimmunoglobulin G (IgG) (H+L) (anti Fc, Listarfish), PE-anti-IL-2 (BD), FITC-anti- IFN-g (BD). To detect the IL3z.CAR expression, APC-anti-IL3 (Miltenyi Biotec) was used. To detect the CD33.CCR, a recombinant human sialic acid binding IgLike Lectin 3/Siglec-3/CD33 protein with an Fc, 6His tag at the C-terminus (C-Fc-6His, Gentaur) was employed, before proceeding with secondary staining with a FITC-anti-His tag (Thermo Fisher Scientific). Briefly, single or Dual CAR-CIKs were incubated 20 minutes at room temperature with CD33 Fc chimera protein (1μg/ml). Cells were washed and then stained at 4°C for 30 minutes with (FITC)-anti-His tag secondary antibody. Unmanipulated CIK-cells were used as negative control.

Antibodies for phenotypic analysis of residual CD34+CD38+ HSPCs after exposure with different CIK conditions included CD123 (BD) and CD45RA (BD) as indicated in supplemental figure 5 (CMP: CD123+/CD45RA-; GMP: CD123+/CD45RA+; MEP: CD123-/CD45-).

Cell death and apoptosis were detected using the GFP-Certified Apoptosis/Necrosis detection kit (Enzo Life Sciences), according to the manufacturer's instructions. Cell membrane labeling was also performed using two lipophilic fluorescent dyes: FITC- and PE-Cell Tracker (Invitrogen).

Human grafts in mice were assessed using PO-anti-human CD45 (Thermo FisherScientific), PerCP-anti-CD3, PeCy7-anti-CD33 (BD), APC-anti-CD123 (BD) and anti-mouse CD45 (eBioscience, San Diego,CA, USA) mAbs. Antibodies for HSPCs subsetting phenotypic analysis included CD45RA-FITC (BD), CD123-APC (BD), CD38-PE-Cy7 (BioLegend), CD34-APC-Cy7 (BioLegend).

Flow cytometry was performed on a FACSCanto II flow cytometer (BD), and data were analyzed using BD FACSDiva software v.8.1.3 and FlowJo v.10.8.1.

Short- and Long-Term Cytotoxicity Assays

To evaluate the killing ability of both unmodified and CAR-redirected CIK cells, short-term cytotoxicity assays were performed. In the short-term cytotoxic assay assessed by means of the double target challenge, CIK cells were co-cultured for 4 hrs with the targets at an effector-target (E:T) ratio of 5:1. Target cells were previously labelled with PE or FITC-Cell Trackers. At the end of the incubation, target cell killing was measured through apoptosis detection by flow cytometry, after annexin V and Necrosis Detection Reagent (NDR) staining. The percentage of killed cells was determined adding the percentage of PE+/Annexin V+/NDR− cells to that of PE+/AnnexinV+/NDR+ cells in co-culture with the effectors compared to target cells alone. Long-term cytotoxicity assays were conducted at an E:T ratio of 1:10 or 1:100, by co-culturing CIK cells with THP-1 or KG-1 AML

cell lines (previously labelled with PE-Cell Trackers) for 1 week. At the end of the culture cells were harvested and flow cytometry-based quantitative analysis was employed to determine the percentage of viable target cells recovered from the culture.

Cytokine Detection

CAR-CIK cell ability to produce cytokines was evaluated following stimulation with the various target cell conditions at an E:T ratio of 1:3. After a 2 hrs and 30 min co-culture, BD GolgiStop was added (BD). The co-culture was then maintained for an additional period of 2 hr and 30 min, after which the cells were collected and stained for anti-CD3 and anti-Fc surface molecule detection. Finally, intracellular cytokine staining (ICS) for IL-2 was performed using the BDCytofix/Cytoperm kit, according to the manufacturer's protocol. Specimens were then analyzed by flow cytometry. The cytokines GM-CSF, IFNγ, IL-2 and TNFα were measured by the Human Singleplex Magnetic Bead Kit (Millipore). The procedure was performed according to the manufacturer's instructions and the concentration was reported in pg/mL.

3D Structure selection, preparation, and mutation

The crystal structure of the human ILR3⟨:IL3 complex (PDB:5UV8; 2.7 Å resolution) was obtained from the RCSB Protein Data Bank [5] and cleaned removing unwanted molecules retaining only the amino acids residues. The missing residues were added to the structure and modelled using MODELLER 9.21 [6]. The structure was used as a template to develop five different mutant models of IL3 bound to its receptor. The five mutated structures N18K, E22R, E43N, F113A, and Mut4 (with the combination of all four mutations), were generated through the FoldX software [7] and used for further analysis.

Molecular Dynamics simulations

To further understand the consequences of mutations on the IL3 structure, all-atom MD simulations were run for 30ns under specified water solvent conditions for WT and its mutants (N18K, E22R, E43N, F113A, and Mut4). The WT and Mut4 were extended to 100ns under the same condition. MD simulations were performed at 300K using the DESAMBER force field [8] and GROMACS 2020.5 software package [9]. All systems were solvated in a periodic cubic box, hydrated with a TIP4PD water model [10], and neutralized with a 0.15 M NaCl solution. The box dimensions were chosen to provide at least 12 Å buffers of solvent molecules around the solute. All systems were minimized using 5000 steps of steepest descent to remove clashes between atoms. After minimization, all systems were equilibrated at a constant temperature of 300K for 125 ps, by utilizing the two-step ensemble process:

NVT (constant number of particles, constant volume, and temperature; Berendsen thermostat with no pressure coupling) and then NPT (constant number of particles, constant pressure, and temperature; Parrinello–Rahman method pressure of 1atm). After the equilibration, the final simulations were performed completely unrestrained at a temperature of 300K and using the linear constraint solver (LINCS) and particle mesh Ewald (PME) algorithms.

Analysis of MD Trajectories

To study the stability of the ILR3⟨:IL3 complex over the simulation time, various analytical methods were employed. All the trajectory files were analyzed to extract the root-mean-square deviation (RMSD), and radius of gyration (Rg), by using gmx rmsd, and gmx gyrate module, respectively, embedded in the GROMACS simulation package. The study of hydrogen bonds was conducted with the Visual Molecular Dynamics software (Theoretical and Computational Biophysics Group at the Beckman Institute for Advanced Science and Technology, University of Illinois, Urbana-Champaign) with a cut-off of 3.0 Å distance. For the study of the free binding energies in all ILR3⟨:IL3 complexes, gmx_MMPBSA was used [11]. According to the MM/GBSA method, binding free energy (ΔGbinding) is calculated by subtracting the free energies of the unbound receptor and ligand from the free energy of the bound complex:

$$\Delta G_{binding,solvated} = G_{complex,solvated} - (G_{protein,solvated} + G_{ligand,solvated})$$

The pictorial structure representations were prepared using Maestro (Schrödinger, LLC, New York City, NY, USA). All the graphs were plotted using the Prism 9 tool.

Mutagenesis of the IL3 sequence

Mutagenesis was performed by overlapping PCR using specific mutated primers synthesized by Eurofins and used to generate protein variants. The mutated IL3z.CAR was then cloned and colonies obtained from the transformations were used for DNA amplification and extraction with the QIAGEN Maxi or Mini Prep Kit. The sequence was verified by DNA sequencing (Eurofins) and the verified plasmids were used for retroviral supernatant production.

Operetta CLS Image Acquisition

Operetta CLS (PerkinElmer) is a high throughput spinning disk confocal microscope equipped with eight emission LED sources ranging from the near ultraviolet 360nm to the far red 650nm working at controlled temperature and CO2 concentration. The confocal images acquisition was performed

using the 40X water immersion objective (numerical aperture 1.1). Target cells were labeled with CellTracker™ Deep Red Dye (ThermoFisher Scientific), CAR-CIK cells were stained with CellTrace™ Violet (ThermoFisher Scientific) and the cell death marker NucView® 488 Green Caspase-3 (Biotium) was used to measure the cytotoxic activity of CAR-CIK cells against target cells.

Cell Avidity Analysis

Cell–cell interaction strength between CAR-CIK cells and OCI-AML3 cells were analyzed using the z-Movi® Cell Avidity Analyzer (LUMICKS, Amsterdam, The Netherlands) with z-Movi microfluidic chips. The microfluidic chips were coated with poly-L-lysine (Sigma-Aldrich) for 10 min and air-dried for 60 min at 37°C. OCI-AML WT, CD33 negative or double negative target cells were concentrated to $1x10^8$ cells/mL and flushed onto separate chips and incubated for 2 hours at 37°C, after which Dual CAR and unmodified CIK cells were fluorescently labeled with CellTrace Far Red dye (Thermo Fisher Scientific) according to the manufacturer's protocol. The chips were transferred onto the z-Movi Cell Avidity Analyzer at 37°C followed by flushing in $1x10^5$ labelled CAR CIK cells and co-incubated with the adhered AML target cells for 5 minutes. Subsequently, a linear force ramp was applied from 0 to 1000 pN (as calibrated for 10 μm polystyrene beads) for 2 min 30 s. CART cell adhesion and detachment was tracked by changes in the z-position and avidity runs were analyzed using Oceon 1.2.8 Software (LUMICKS).

Mice

Immunocompromised NSG mice were purchased (The Jackson Laboratory) and bred in-house under pathogen-free conditions. Procedures involving animal handling and care were conformed to protocols approved by both Milano-Bicocca and Perugia University in compliance with national and international law and policies. For the OCI-AML3 model, 8- to 12-week-old mice received an intravenous injection via tail vein of 1×10^6 OCI-AML3 wt or KO clones stably expressing luciferase, monitoring leukemia progression every week by Bioluminescence imaging using an IVIS Lumina III imaging system and Living Image software (PerkinElmer, USA) for analysis. For the KG-1 model, 8- to 12-week-old mice received a radiation dose of 0.9 Gy followed 24 hours later by an intravenous injection via tail vein of $2,5 \times 10^6$ KG-1 cells stably expressing luciferase. CAR-CIK cells were then injected via tail vein at a time and dose provided in the figure legends. In experiments addressing low affinity Dual CAR-CIK cells efficacy, leukemia progression was measured by Bioluminescence imaging using an IVIS Lumina III imaging system and analyzed with Living Image software (PerkinElmer, USA). In experiments addressing Dual CAR-CIK cells design optimization, leukemia progression was measured by phenotypic analysis of PB bleeding, performed every week.

Statistical Analysis

Categorical variables are described by counts and percentages, and quantitative characteristics are expressed as median (I-III quartile) or mean (standard deviation, SD), as appropriate. The Wilcoxon signed-rank test or the Tukey's test were used for comparing quantitative variables between two paired or unpaired samples, respectively. The Kaplan-Meier method was applied to estimate survival curves, while the log-rank test for comparisons. P-values were adjusted for multiple testing using the Benjamini-Hochberg method. Analyses were performed using R 4.2.1 (R Foundation for Statistical Computing, Vienna, Austria) and GraphPad Prism (La Jolla, CA, USA) softwares. P-values are denoted with asterisks as follows: p-value > 0.05, not significant (ns); *, p-value < 0.05; **, p-value < 0.01; ***, p-value < 0.001; ****, p-value < 0.0001.

Supplemental Table 1. CD123 sgRNA off-targeted analysis

Chrom	Strand	Start	End	Actual genomic hit	Number of mismatches	Pre-mRNA (Unspliced)	mRNA (CDS)
X	-	1471083	1471105	G**t**CGTACTGGACGTCCGCGG-GGG	1	IL3RA - interleukin 3 receptor, alpha (low affinity)	IL3RA - interleukin 3 receptor, alpha (low affinity)
Y	-	1421083	1421105	G**t**CGTACTGGACGTCCGCGG-GGG	1	-	-
7	-	151328949	151328971	GG**g**GTAC**c**GG**g**CGTCCGCGG-AGG	3	PRKAG2 - protein kinase, AMP-activated, gamma 2 non-catalytic subunit	-
1	+	1580063	1580085	**ct**CGTACTGG**c**CG**g**CCGCGG-TGG	4	CDK11B - cyclin-dependent kinase 11B	-
1	+	1643278	1643300	**ct**CGTACTGG**c**CG**g**CCGCGG-TGG	4	CDK11A - cyclin-dependent kinase 11A	-
9	-	134471732	134471754	G**a**CG**gg**C**c**GGACGTCCGCGG-AGG	4	RAPGEF1 - Rap guanine nucleotide exchange factor (GEF) 1	RAPGEF1 - Rap guanine nucleotide exchange factor (GEF) 1
2	+	219846632	219846654	G**c**CGT**c**CTGG**g**CG**g**CCGCGG-CGG	4	FEV - FEV (ETS oncogene family)	FEV - FEV (ETS oncogene family)
3	+	195589773	195589795	GG**g**G**a**A**g**TGGACG**g**CCGCGG-TGG	4	-	-
7	+	128573480	128573502	GG**t**GT**c**CTGGA**g**G**c**CCGCGG-GGG	4	-	-
11	+	65453682	65453704	GG**a**GTACTGG**c**CG**gg**CGCGG-TGG	4	-	-
15	-	76604565	76604587	GGC**a**TACTGG**c**CG**gg**CGCGG-TGG	4	-	-

Chrom	Strand	Start	End	Actual genomic hit	Number of mismatches	Pre-mRNA (Unspliced)	mRNA (CDS)
8	+	58129538	58129560	GGCG**gtag**GGACGTCCGCGG-CGG	4	-	-
2	-	157190414	157190436	GGCG**act**TGGACG**g**CCGCGG-GGG	4	**NR4A2 - nuclear receptor subfamily 4, group A, member 2**	-
22	-	37948437	37948459	GGCG**g**A**g**TGG**gg**GTCCGCGG-TGG	4	-	-
10	-	83634281	83634303	GGCG**c**AC**c**GG**g**CG**c**CCGCGG-CGG	4	-	-
10	+	135278760	135278782	GGCG**c**ACTG**cg**CGT**g**CGCGG-GGG	4	**SPRN - shadow of prion protein homolog (zebrafish)**	-
19	-	39342698	39342720	GGCGT**c**C**g**GG**c**CG**g**CCGCGG-GGG	4	**HNRNPL - heterogeneous nuclear ribonucleoprotein L**	-
17	-	7906865	7906887	GGCGTA**ga**GG**g**C**a**TCCGCGG-CGG	4	**GUCY2D - guanylate cyclase 2D, membrane (retina-specific)**	**GUCY2D - guanylate cyclase 2D, membrane (retina-specific)**
9	-	140570657	140570679	GGCGTA**a**TGG**c**CG**gg**CGCGG-TGG	4	**EHMT1 - euchromatic histone-lysine N-methyltransferase 1**	-

Number of potential off-targets for the predicted CD123 sgRNA shown through the Off-Spotter algorithm (https://cm.jefferson.edu/Off-Spotter/) together with genomic location information and annotation (ENSEMBL gene identifiers, transcript identifiers and common gene names). Mismatches are indicated by red lowercase letters for each off-target.

Supplemental Table 2. CD33 sgRNA off-targeted analysis

Chrom	Strand	Start	End	Genomic hit	Number of mismatches	Pre-mRNA (Unspliced)	mRNA (CDS)
19	-	51729087	51729109	GGCCGGGTTCTAGAGTGCCA-GGG	0	CD33 molecule	CD33 molecule
7	+	86828849	86828871	GGatGGGTcCTAGAGTGCCA-AGG	3	TMEM243 - transmembrane protein 243, mitochondrial	-
12	+	102520020	102520042	aaCtaGGTTCTAGAGTGCCA-GGG	4	PARPBP - PARP1 binding protein	-
5	+	85854213	85854235	tGCatGGTgCTAGAGTGCCA-TGG	4	-	-
8	-	53853799	53853821	aGCCaGGTTCcAGAcTGCCA-GGG	4	-	-
2	+	20601632	20601654	tGCCaGGTTCTgGcGTGCCA-TGG	4	-	-
19	+	13616844	13616866	GatgGGGTTgTAGAGTGCCA-TGG	4	CACNA1A - calcium channel, voltage-dependent, P/Q type, alpha 1A subunit	CACNA1A - calcium channel, voltage-dependent, P/Q type, alpha 1A subunit
8	+	140607489	140607511	GcCtGaGTTCaAGAGTGCCA-GGG	4	-	-
7	+	140772808	140772830	GaCgGGGTgCcAGAGTGCCA-AGG	4	-	-
1	-	239501285	239501307	GtCaGGGTTCTAtAaTGCCA-AGG	4	-	-
15	+	71624385	71624407	GGaaGGGTcCTAGAtTGCCA-AGG	4	(THSD4 - thrombospondin, type I, domain containing 4	-
8	+	62856457	62856479	GGttGGGTTtTtGAGTGCCA-TGG	4	-	-
4	-	102442679	102442701	GGaCtGGaaCTAGAGTGCCA-TGG	4	BANK1 - B-cell scaffold protein	-

Chrom	Strand	Start	End	Genomic hit	Number of mismatches	Pre-mRNA (Unspliced)	mRNA (CDS)
						with ankyrin repeats 1	
18	+	68387779	68387801	GGC**t**GGG**g**TCT**gc**AGTGCCA-GGG	4	-	-
9	-	79634638	79634660	GGCCG**a**GT**g**CT**g**GA**t**TGCCA-TGG	4	FOXB2 - forkhead box B2	FOXB2 - forkhead box B2
20	-	34652614	34652636	GGCCGG**c**T**c**C**c**AGA**c**TGCCA-GGG	4	-	-
2	+	134344765	134344787	GGCCGGG**ag**C**c**AGA**t**TGCCA-GGG	4	-	-

Number of potential off-targets for the predicted CD33 sgRNA shown through the Off-Spotter algorithm (https://cm.jefferson.edu/Off-Spotter/) together with genomic location information and annotation (ENSEMBL gene identifiers, transcript identifiers and common gene names). Mismatches are indicated by red lowercase letters for each off-target.

Supplemental Table 3. OCI-AML3 CD33 KO vs WT heatmap path

Genes	Pathway	log2 Fold Change	P adj	OCI AML3 wt_1	OCI AML3 wt_2	OCI AML3 wt_3	OCI AML3 33 KO_1	OCI AML3 33 KO_2	OCI AML3 33 KO_3
NOTCH3	MicroRNAs in cancer	-6,035209366	2,78E-30	0,151065887	0,144365548	0,126965717	0,002003954	0	0,002167463
ZEB1	MicroRNAs in cancer	-5,819443464	5,52E-108	0,994357278	0,829792336	0,920956757	0,005063049	0,013600178	0,024642724
EFNA2	MicroRNAs in cancer	-4,994753534	2,65E-27	0,808880653	0,734353574	0,493835875	0,037754225	0	0,008166945
CYP1B1	MicroRNAs in cancer	-4,244411692	2,92E-51	0,772096702	0,584132293	0,609418435	0,015693683	0,044966188	0,037343208
THBS1	MicroRNAs in cancer	-3,443317772	1,05E-30	0,60957097	0,44943397	0,37109655	0,041901321	0,020009565	0,048341542
IRS1	MicroRNAs in cancer	-3,341375747	1,17E-171	2,622380708	2,647517238	2,569267204	0,251791638	0,172403843	0,268331252
PDGFA	MicroRNAs in cancer	-2,954271957	5,58E-60	2,24039097	1,833340455	2,037303892	0,207431691	0,247642428	0,261749561
TIMP3	MicroRNAs in cancer	-2,574401337	9,98E-308	102,6084129	98,63061295	104,7781989	16,29773495	15,516723	15,500614
FGFR3	MicroRNAs in cancer	-2,550576886	9,25E-32	0,650676866	0,735125765	0,603322949	0,094754767	0,130526569	0,098544365
HMOX1	MicroRNAs in cancer	-2,206109861	1,10E-06	0,322873955	0,696173346	0,706860831	0,213617678	0,054648765	0,066013568
FZD3	MicroRNAs in cancer	-2,004189619	2,18E-31	0,381666663	0,387349124	0,302101509	0,08211893	0,081931528	0,081206218
TPM1	MicroRNAs in cancer	-1,819804328	3,34E-25	1,456258909	1,925141236	1,638494791	0,357381109	0,527558849	0,47011753
ST14	MicroRNAs in cancer	-1,664020984	1,28E-17	0,719495256	0,812091205	0,90153106	0,26466398	0,219423073	0,222645763
PTGS2	MicroRNAs in cancer	-1,526094871	1,93E-11	0,48560444	0,427896207	0,382577169	0,147591878	0,109589445	0,140166802
PLAU	MicroRNAs in cancer	1,710703399	1,54E-40	2,194702699	1,783135448	2,224223471	6,217034512	5,782001901	6,360125106
IGF2BP1	MicroRNAs in cancer	2,020441789	9,98E-308	2,985728017	3,036176714	2,759390313	11,118295	10,46054273	11,2055567
VEGFA	MicroRNAs in cancer	2,116538748	2,51E-302	12,28051258	12,77846922	13,00196463	46,82642311	54,93777605	50,74902282
TNN	MicroRNAs in cancer	2,708249861	1,67E-120	0,743196788	0,818196836	0,752476005	4,741074228	4,800317869	4,544562285
CDKN2A	MicroRNAs in cancer	3,876975738	9,98E-308	5,898315164	4,560515532	3,467872125	60,51595259	59,65604397	61,3875358
DDIT4	MicroRNAs in cancer	4,256779658	9,98E-308	12,67307915	13,28999268	13,15075845	212,1348605	243,3492054	235,7940987
RASGRP4	Ras signaling pathway	-5,689897978	8,47E-138	2,273311569	2,926815587	2,691332625	0,020104301	0,063004015	0,065234042
HTR7	Ras signaling pathway	-5,303530055	4,31E-30	0,268098114	0,515769004	0,512957094	0,009653184	0,008643344	0,010440821
EFNA2	Ras signaling pathway	-4,994753534	2,65E-27	0,808880653	0,734353574	0,493835875	0,037754225	0	0,008166945
BDNF	Ras signaling pathway	-4,808976873	3,81E-38	0,282290173	0,389446721	0,256613835	0,008370506	0	0,018106969
VEGFC	Ras signaling pathway	-3,749092507	8,75E-99	3,164017925	3,737035931	3,59202658	0,193560434	0,291163599	0,259598595
GNG11	Ras signaling pathway	-3,515808697	3,13E-106	16,68182099	15,04304394	14,13721663	1,135903526	1,700183812	0,971866424
TGFA	Ras signaling pathway	-3,424260963	4,63E-42	0,774223276	0,66233808	0,682597763	0,075052946	0,073921648	0,032470711
PDGFA	Ras signaling pathway	-2,954271957	5,58E-60	2,24039097	1,833340455	2,037303892	0,207431691	0,247642428	0,261749561
PAK6	Ras signaling pathway	-2,796774165	7,02E-12	0,210225056	0,163022617	0,291034802	0,019869668	0,041512473	0,028654538
FGFR3	Ras signaling pathway	-2,550576886	9,25E-32	0,650676866	0,735125765	0,603322949	0,094754767	0,130526569	0,098544365
GNG2	Ras signaling pathway	-2,513274929	8,40E-52	1,453182055	1,469211079	1,420580338	0,274698418	0,186334571	0,220583167
FGFR1	Ras signaling pathway	-2,326322276	1,26E-38	1,007924584	1,136890715	1,520907548	0,233511947	0,183809904	0,249789562
GNG12	Ras signaling pathway	-2,202338942	5,82E-57	2,110415918	1,792643665	1,791884144	0,38151205	0,381016795	0,361060831
CSF1R	Ras signaling pathway	-2,084433348	2,37E-58	3,589885545	3,065994133	3,616285705	0,784165199	0,76334352	0,669819425
HGF	Ras signaling pathway	-1,882377412	1,46E-53	5,512371859	4,73250081	5,015520605	1,38558005	1,176402694	1,212791294
GNG7	Ras signaling pathway	-1,612850209	9,27E-32	1,692692942	2,250218927	1,985236791	0,624710604	0,53207253	0,642722779
GNG4	Ras signaling pathway	1,614371178	3,65E-40	0,77314697	0,647075357	0,740527208	1,957798205	1,952006164	2,048384128
RRAS2	Ras signaling pathway	1,988135578	5,97E-57	1,002674976	1,065536125	1,165132802	4,10224895	4,030942181	3,769513886

PDGFC	Ras signaling pathway	2,111659615	1,14E-46	0,920017183	0,828922766	1,30328863	4,258233692	4,001521849	3,796264156
VEGFA	Ras signaling pathway	2,116538748	2,51E-302	12,28051258	12,77846922	13,00196463	46,82642311	54,93777605	50,74902282
RASGRP4	MAPK signaling pathway	-5,689897978	8,47E-138	2,273311569	2,926815587	2,691332625	0,020104301	0,063004015	0,065234042
EFNA2	MAPK signaling pathway	-4,994753534	2,65E-27	0,808880653	0,734353574	0,493835875	0,037754225	0	0,008166945
BDNF	MAPK signaling pathway	-4,808976873	3,81E-38	0,282290173	0,389446721	0,256613835	0,008370506	0	0,018106969
MAP2K6	MAPK signaling pathway	-4,62661573	7,82E-67	1,751059991	1,880654138	1,750967228	0,103845328	0,015496975	0,056159216
CD14	MAPK signaling pathway	-3,852050901	8,58E-58	2,345126855	2,043033629	2,635705425	0,179113066	0,080187834	0,154982021
HSPA2	MAPK signaling pathway	-3,768753437	8,94E-92	2,085737762	2,279292522	2,292083302	0,181073025	0,125520458	0,132670823
VEGFC	MAPK signaling pathway	-3,749092507	8,75E-99	3,164017925	3,737035931	3,59202658	0,193560434	0,291163599	0,259598595
NFATC1	MAPK signaling pathway	-3,613310103	8,62E-162	4,707627254	4,390601548	4,253998427	0,314500634	0,373760073	0,324699937
TGFA	MAPK signaling pathway	-3,424260963	4,63E-42	0,774223276	0,66233808	0,682597763	0,075052946	0,073921648	0,032470711
PDGFA	MAPK signaling pathway	-2,954271957	5,58E-60	2,24039097	1,833340455	2,037303892	0,207431691	0,247642428	0,261749561
MAPK11	MAPK signaling pathway	-2,641543045	6,15E-18	0,659925941	0,663029412	0,503116881	0,099797881	0,107229375	0,064764443
FGFR3	MAPK signaling pathway	-2,550576886	9,25E-32	0,650676866	0,735125765	0,603322949	0,094754767	0,130526569	0,098544365
IL1B	MAPK signaling pathway	-2,411264962	3,67E-81	14,95043276	18,9917713	18,97748961	3,303882797	2,764906494	3,094661445
MAP4K1	MAPK signaling pathway	-2,348772492	5,00E-228	17,59459247	20,40021925	20,16048299	3,727131442	3,38872874	3,427799145
FGFR1	MAPK signaling pathway	-2,326322276	1,26E-38	1,007924584	1,136890715	1,520907548	0,233511947	0,183809904	0,249789562
GNG12	MAPK signaling pathway	-2,202338942	5,82E-57	2,110415918	1,792643665	1,791884144	0,38151205	0,381016795	0,361060831
MEF2C	MAPK signaling pathway	-2,164101895	4,38E-146	7,469811712	7,38136132	6,886695599	1,566965339	1,324977788	1,541903462
CSF1R	MAPK signaling pathway	-2,084433348	2,37E-58	3,589885545	3,065994133	3,616285705	0,784165199	0,76334352	0,669819425
HGF	MAPK signaling pathway	-1,882377412	1,46E-53	5,512371859	4,73250081	5,015520605	1,38558005	1,176402694	1,212791294
IL1R1	MAPK signaling pathway	-1,769965655	1,27E-12	0,277902008	0,321770356	0,392117633	0,088315456	0,070896252	0,105402949
FOS	MAPK signaling pathway	1,710991908	2,20E-28	44,06937728	57,69178774	50,91687008	105,5426317	182,9634587	172,4067618
DDIT3	MAPK signaling pathway	1,783843112	1,43E-73	6,428014789	6,857845562	6,790819701	21,47368004	21,24343178	21,31011014
JUN	MAPK signaling pathway	1,784371902	4,61E-182	12,68747439	11,86913973	10,91260438	34,24118452	39,69345564	38,13003708
RRAS2	MAPK signaling pathway	1,988135578	5,97E-57	1,002674976	1,065536125	1,165132802	4,10224895	4,030942181	3,769513886
PDGFC	MAPK signaling pathway	2,111659615	1,14E-46	0,920017183	0,828922766	1,30328863	4,258233692	4,001521849	3,796264156

VEGFA	MAPK signaling pathway	2,116538748	2,51E-302	12,28051258	12,77846922	13,00196463	46,82642311	54,93777605	50,74902282
CD14	Hematopoietic cell lineage	-3,852050901	8,58E-58	2,345126855	2,043033629	2,635705425	0,179113066	0,080187834	0,154982021
CR1	Hematopoietic cell lineage	-3,521888721	8,92E-165	2,311605484	1,993399804	2,398112423	0,186634521	0,171469686	0,17377744
CD36	Hematopoietic cell lineage	-2,785461868	9,98E-308	15,57277841	16,02374142	16,59811654	2,202417435	2,081426166	2,143585977
ITGA6	Hematopoietic cell lineage	-2,617343249	7,60E-47	0,93882132	0,885746412	0,859118239	0,147541691	0,164510655	0,096350269
IL1B	Hematopoietic cell lineage	-2,411264962	3,67E-81	14,95043276	18,9917713	18,97748961	3,303882797	2,764906494	3,094661445
CD37	Hematopoietic cell lineage	-2,409961359	9,98E-308	130,9237002	132,2343201	125,6026902	22,17243964	23,16175589	22,2223552
CSF1R	Hematopoietic cell lineage	-2,084433348	2,37E-58	3,589885545	3,065994133	3,616285705	0,784165199	0,76334352	0,669819425
IL1R1	Hematopoietic cell lineage	-1,769965655	1,27E-12	0,277902008	0,321770356	0,392117633	0,088315456	0,070896252	0,105402949
FCER2	Hematopoietic cell lineage	3,339557689	1,21E-75	0,633513574	0,360874746	0,460712737	4,35812671	3,616275734	4,348001703
PTK2	Trans misreg in cancer	-6,036945062	1,30E-307	4,617028414	4,802913489	4,700059147	0,076194008	0,068223191	0,052443327
ZEB1	Trans misreg in cancer	-5,819443464	5,52E-108	0,994357278	0,829792336	0,920956757	0,005063049	0,013600178	0,024642724
MEIS1	Trans misreg in cancer	-5,541029076	3,06E-300	10,3488918	10,14017905	9,965682862	0,157620625	0,2549474	0,208977251
WT1	Trans misreg in cancer	-4,85250235	5,52E-193	4,376189155	3,885086429	3,870181619	0,156175352	0,078658603	0,126688683
CD14	Trans misreg in cancer	-3,852050901	8,58E-58	2,345126855	2,043033629	2,635705425	0,179113066	0,080187834	0,154982021
IGFBP3	Trans misreg in cancer	-3,834456472	1,19E-68	2,097576233	2,635038885	2,726409022	0,153685955	0,275217081	0,093086408
PDGFA	Trans misreg in cancer	-2,954271957	5,58E-60	2,24039097	1,833340455	2,037303892	0,207431691	0,247642428	0,261749561
ITGB7	Trans misreg in cancer	-2,723765492	9,99E-41	1,432492746	1,429204657	1,510413043	0,191807791	0,121229909	0,268475134
CD86	Trans misreg in cancer	-2,168976248	2,56E-12	0,57099629	0,42534313	0,384636797	0,083028285	0,128860367	0,071842282
MEF2C	Trans misreg in cancer	-2,164101895	4,38E-146	7,469811712	7,38136132	6,886695599	1,566965339	1,324977788	1,541903462
CSF1R	Trans misreg in cancer	-2,084433348	2,37E-58	3,589885545	3,065994133	3,616285705	0,784165199	0,76334352	0,669819425
BAIAP3	Trans misreg in cancer	-2,079302477	3,83E-15	0,353699519	0,359338542	0,396933951	0,108250578	0,074120077	0,055097939
MITF	Trans misreg in cancer	-1,94648696	1,93E-31	1,368704808	1,057801148	1,144355259	0,329050833	0,213842995	0,27840505
PBX1	Trans misreg in cancer	-1,596404112	1,60E-39	1,227089411	1,178733998	1,144490394	0,356139983	0,331470927	0,380130283
CDKN2C	Trans misreg in cancer	1,70237418	1,04E-275	14,11352025	13,69087683	12,75289296	41,90335011	40,25483632	38,85583147
PLAU	Trans misreg in cancer	1,710703399	1,54E-40	2,194702699	1,783135448	2,224223471	6,217034512	5,782001901	6,360125106
DDIT3	Trans misreg in cancer	1,783843112	1,43E-73	6,428014789	6,857845562	6,790819701	21,47368004	21,24343178	21,31011014
BIRC3	Trans misreg in cancer	1,969599564	6,02E-17	0,046420138	0,078667249	0,105213405	0,320576629	0,293325983	0,268275628
CCNA1	Trans misreg in cancer	4,082678093	2,98E-100	0,223010247	0,236206787	0,344633941	4,335057519	4,617607017	3,708459892
CD226	Cell adhesion molecules	-4,100672117	5,74E-39	0,892092657	0,719910001	0,612718051	0,044969166	0,02684323	0,037829833
CADM1	Cell adhesion molecules	-3,492762542	2,25E-31	0,467336903	0,517089203	0,42128898	0,047851804	0,006591681	0,047774954
SDC2	Cell adhesion molecules	-2,794548237	9,98E-308	37,6556961	38,13145858	38,54810571	5,197928003	4,986601833	4,974505962
ITGB7	Cell adhesion molecules	-2,723765492	9,99E-41	1,432492746	1,429204657	1,510413043	0,191807791	0,121229909	0,268475134
ITGA6	Cell adhesion molecules	-2,617343249	7,60E-47	0,93882132	0,885746412	0,859118239	0,147541691	0,164510655	0,096350269
CLDN23	Cell adhesion molecules	-2,538214294	3,62E-39	2,202597489	2,069298686	2,015205188	0,40600491	0,296760714	0,26885649
CD86	Cell adhesion molecules	-2,168976248	2,56E-12	0,57099629	0,42534313	0,384636797	0,083028285	0,128860367	0,071842282
JAM2	Cell adhesion molecules	-1,591550608	2,07E-10	0,453458148	0,486528899	0,339763312	0,15585138	0,124042166	0,108632607
HLA-A	Cell adhesion molecules	1,500948063	4,86E-29	14,54905664	18,58028755	14,15299304	47,35210804	30,59542168	45,45375831
ICAM2	Cell adhesion molecules	1,539306295	2,55E-30	1,390446192	1,772370682	1,432505033	4,332866211	4,278966035	4,112086171
HLA-B	Cell adhesion molecules	1,661902278	9,20E-84	42,46103157	34,45779917	31,47552833	106,0238205	106,7504417	103,3461241

HLA-C	Cell adhesion molecules	1,761752542	1,72E-45	19,84412887	12,26175654	15,93441671	47,64374672	53,44147907	48,99251361
HLA-F	Cell adhesion molecules	3,078794235	2,70E-17	0,022534	0,057963783	0,026117571	0,217242403	0,233927996	0,469935938
JAK3	PI3K-Akt signaling pathway	-8,974264881	1,10E-127	0,980163687	0,925592422	0,942896858	0,002976428	0	0
PRL	PI3K-Akt signaling pathway	-6,099162572	1,63E-43	1,234909662	1,107783161	1,13594979	0	0	0,036069269
PTK2	PI3K-Akt signaling pathway	-6,036945062	1,30E-307	4,617028414	4,802913489	4,700059147	0,076194008	0,068223191	0,052443327
COL6A2	PI3K-Akt signaling pathway	-5,887535352	1,85E-236	4,019936893	4,906326762	4,309022249	0,081949797	0,026682493	0,080578515
ITGB5	PI3K-Akt signaling pathway	-5,73179401	1,95E-188	2,725078292	2,407494921	2,716942921	0,055390102	0,0132255	0,051921631
EFNA2	PI3K-Akt signaling pathway	-4,994753534	2,65E-27	0,808880653	0,734353574	0,493835875	0,037754225	0	0,008166945
BDNF	PI3K-Akt signaling pathway	-4,808976873	3,81E-38	0,282290173	0,389446721	0,256613835	0,008370506	0	0,018106969
LAMA5	PI3K-Akt signaling pathway	-4,72477332	9,87E-84	0,376123725	0,372048494	0,352799313	0,016978997	0,010135192	0,009182186
VEGFC	PI3K-Akt signaling pathway	-3,749092507	8,75E-99	3,164017925	3,737035931	3,59202658	0,193560434	0,291163599	0,259598595
GNG11	PI3K-Akt signaling pathway	-3,515808697	3,13E-106	16,68182099	15,04304394	14,13721663	1,135903526	1,700183812	0,971866424
THBS1	PI3K-Akt signaling pathway	-3,443317772	1,05E-30	0,60957097	0,44943397	0,37109655	0,041901321	0,020009565	0,048341542
TGFA	PI3K-Akt signaling pathway	-3,424260963	4,63E-42	0,774223276	0,66233808	0,682597763	0,075052946	0,073921648	0,032470711
IRS1	PI3K-Akt signaling pathway	-3,341375747	1,17E-171	2,622380708	2,647517238	2,569267204	0,251791638	0,172403843	0,268331252
PDGFA	PI3K-Akt signaling pathway	-2,954271957	5,58E-60	2,24039097	1,833340455	2,037303892	0,207431691	0,247642428	0,261749561
IL2RG	PI3K-Akt signaling pathway	-2,875492074	5,10E-32	1,673303742	1,519132122	1,702369603	0,179241505	0,28321883	0,171058627
ITGB7	PI3K-Akt signaling pathway	-2,723765492	9,99E-41	1,432492746	1,429204657	1,510413043	0,191807791	0,121229909	0,268475134
FN1	PI3K-Akt signaling pathway	-2,68895037	3,29E-161	6,442144829	5,357421837	6,39023966	0,933491402	0,806792358	0,838133273
ITGA6	PI3K-Akt signaling pathway	-2,617343249	7,60E-47	0,93882132	0,885746412	0,859118239	0,147541691	0,164510655	0,096350269
FGFR3	PI3K-Akt signaling pathway	-2,550576886	9,25E-32	0,650676866	0,735125765	0,603322949	0,094754767	0,130526569	0,098544365
GNG2	PI3K-Akt signaling pathway	-2,513274929	8,40E-52	1,453182055	1,469211079	1,420580338	0,274698418	0,186334571	0,220583167
FGFR1	PI3K-Akt signaling pathway	-2,326322276	1,26E-38	1,007924584	1,136890715	1,520907548	0,233511947	0,183809904	0,249789562
F2R	PI3K-Akt signaling pathway	-2,227794826	1,28E-11	0,589499199	0,463827055	0,425131445	0,152824346	0,053214415	0,064280929
GNG12	PI3K-Akt signaling pathway	-2,202338942	5,82E-57	2,110415918	1,792643665	1,791884144	0,38151205	0,381016795	0,361060831
CSF1R	PI3K-Akt signaling pathway	-2,084433348	2,37E-58	3,589885545	3,065994133	3,616285705	0,784165199	0,76334352	0,669819425
HGF	PI3K-Akt signaling pathway	-1,882377412	1,46E-53	5,512371859	4,73250081	5,015520605	1,38558005	1,176402694	1,212791294

OSMR	PI3K-Akt signaling pathway	-1,743668305	4,98E-172	9,040549519	8,665672163	8,265379121	2,418061363	2,341797834	2,353538896
LPAR1	PI3K-Akt signaling pathway	-1,731847146	1,91E-09	0,405121203	0,570082141	0,615628849	0,12252962	0,237708329	0,115961335
GNG7	PI3K-Akt signaling pathway	-1,612850209	9,27E-32	1,692692942	2,250218927	1,985236791	0,624710604	0,53207253	0,642722779
GNG4	PI3K-Akt signaling pathway	1,614371178	3,65E-40	0,77314697	0,647075357	0,740527208	1,957798205	1,952006164	2,048384128
COL4A1	PI3K-Akt signaling pathway	1,743331296	3,14E-40	0,370185341	0,341288432	0,31929729	1,130481226	0,979190918	1,018543132
PDGFC	PI3K-Akt signaling pathway	2,111659615	1,14E-46	0,920017183	0,828922766	1,30328863	4,258233692	4,001521849	3,796264156
VEGFA	PI3K-Akt signaling pathway	2,116538748	2,51E-302	12,28051258	12,77846922	13,00196463	46,82642311	54,93777605	50,749022822
COL9A2	PI3K-Akt signaling pathway	2,439950421	6,57E-74	0,884025694	0,857451973	0,68891282	3,98206118	4,286771927	3,855882613
TNN	PI3K-Akt signaling pathway	2,708249861	1,67E-120	0,743196788	0,818196836	0,752476005	4,741074228	4,800317869	4,544562285
DDIT4	PI3K-Akt signaling pathway	4,256779658	9,98E-308	12,67307915	13,28999268	13,15075845	212,1348605	243,3492054	235,7940987
BMPR1B	Cytokine-receptor interaction	-8,896698793	2,93E-112	0,723329458	0,89191508	0,800821669	0	0	0,002943068
PRL	Cytokine-receptor interaction	-6,099162572	1,63E-43	1,234909662	1,107783161	1,13594979	0	0	0,036069269
LIFR	Cytokine-receptor interaction	-4,472788499	6,81E-43	0,314594936	0,229607555	0,276447571	0,006218941	0,025057638	0,006726366
CX3CR1	Cytokine-receptor interaction	-4,004267431	1,36E-215	5,404629241	5,681964	6,146615925	0,327281743	0,348484881	0,320500658
TNFRSF11A	Cytokine-receptor interaction	-3,149833812	2,32E-157	7,153419035	7,005928866	7,355404732	0,725413769	0,882851816	0,655105258
IL2RG	Cytokine-receptor interaction	-2,875492074	5,10E-32	1,673303742	1,519132122	1,702369603	0,179241505	0,28321883	0,171058627
IL18RAP	Cytokine-receptor interaction	-2,726061607	6,79E-35	1,201257928	1,403211326	1,348977588	0,248270425	0,097594388	0,176835298
CCL23	Cytokine-receptor interaction	-2,676514165	9,54E-19	4,510435677	2,729907925	2,904293352	0,542575252	0,323876868	0,475065696
IL16	Cytokine-receptor interaction	-2,494298563	8,76E-50	0,684800559	0,745115483	0,673806188	0,114419746	0,145861093	0,094389905
IL1B	Cytokine-receptor interaction	-2,411264962	3,67E-81	14,95043276	18,9917713	18,97748961	3,303882797	2,764906494	3,094661445
CSF1R	Cytokine-receptor interaction	-2,084433348	2,37E-58	3,589885545	3,065994133	3,616285705	0,784165199	0,76334352	0,669819425
GDF15	Cytokine-receptor interaction	-1,968944159	5,24E-13	1,871659956	1,796310437	1,322245555	0,363912973	0,555140375	0,291559927
IL1R1	Cytokine-receptor interaction	-1,769965655	1,27E-12	0,277902008	0,321770356	0,392117633	0,088315456	0,070896252	0,105402949
OSMR	Cytokine-receptor interaction	-1,743668305	4,98E-172	9,040549519	8,665672163	8,265379121	2,418061363	2,341797834	2,353538896
TNFSF12	Cytokine-receptor interaction	-1,71861759	1,19E-52	7,424114041	7,672224867	7,892788852	2,199651747	2,156692507	2,088466187
IL18R1	Cytokine-receptor interaction	-1,711493642	9,19E-42	1,984854176	2,245943003	2,10712881	0,639474114	0,584262621	0,569318201
TNFRSF10C	Cytokine-receptor interaction	-1,568087824	6,41E-25	4,080497896	4,926384135	5,796993565	1,753797459	1,454008316	1,416817317

IL15RA	Cytokine-receptor interaction	1,511673431	1,35E-42	1,944581772	2,591032938	2,915398951	6,722669923	6,615441905	6,764823279
IL18	Cytokine-receptor interaction	1,5271106	7,70E-30	2,349773615	2,895158554	2,420850624	6,345474678	7,676555429	6,95473375
BMP8B	Cytokine-receptor interaction	1,6297523	1,05E-303	46,97610661	47,37799176	46,24179724	132,7349447	136,8355549	131,3897464
EDA2R	Cytokine-receptor interaction	2,134352156	1,37E-54	0,930795627	0,622943044	0,663888982	2,891904113	2,803474042	2,786288176
CCR2	Cytokine-receptor interaction	2,315483531	9,98E-308	8,081879508	7,982577606	8,160186196	37,79482772	35,26455376	37,5909574
IL32	Cytokine-receptor interaction	2,540677417	5,07E-32	0,268948862	0,748784849	0,471043052	3,294434288	3,131882723	2,742080792
INHBE	Cytokine-receptor interaction	3,836996928	5,74E-23	0,078996141	0,031874554	0,040692826	0,477850436	0,701217437	0,574266578
JAK3	Pathways in cancer	-8,974264881	1,10E-127	0,980163687	0,925592422	0,942896858	0,002976428	0	0
ADCY1	Pathways in cancer	-6,060183507	3,18E-25	0,124064648	0,087103487	0,066465054	0,001250786	0,002239877	0
PTK2	Pathways in cancer	-6,036945062	1,30E-307	4,617028414	4,802913489	4,700059147	0,076194008	0,068223191	0,052443327
NOTCH3	Pathways in cancer	-6,035209366	2,78E-30	0,151065887	0,144365548	0,126965717	0,002003954	0	0,002167463
RASGRP4	Pathways in cancer	-5,689897978	8,47E-138	2,273311569	2,926815587	2,691332625	0,020104301	0,063004015	0,065234042
FZD6	Pathways in cancer	-5,458597499	8,50E-41	0,391586261	0,597449338	0,479074476	0,016449438	0	0,008895803
SMO	Pathways in cancer	-5,193372036	2,29E-176	2,489918058	2,556711149	2,512160407	0,069248745	0,069755047	0,051493056
LAMA5	Pathways in cancer	-4,72477332	9,87E-84	0,376123725	0,372048494	0,352799313	0,016978997	0,010135192	0,009182186
CTNNA2	Pathways in cancer	-4,121485015	1,66E-25	0,296963897	0,245093466	0,285086599	0,020413012	0,018277564	0,003679763
RB1	Pathways in cancer	-3,808377037	9,98E-308	15,20905815	15,66343959	15,99468245	1,067640742	1,062169528	0,964127337
VEGFC	Pathways in cancer	-3,749092507	8,75E-99	3,164017925	3,737035931	3,59202658	0,193560434	0,291163599	0,259598595
GNG11	Pathways in cancer	-3,515808697	3,13E-106	16,68182099	15,04304394	14,13721663	1,135903526	1,700183812	0,971866424
TGFA	Pathways in cancer	-3,424260963	4,63E-42	0,774223276	0,66233808	0,682597763	0,075052946	0,073921648	0,032470711
PDGFA	Pathways in cancer	-2,954271957	5,58E-60	2,24039097	1,833340455	2,037303892	0,207431691	0,247642428	0,261749561
IL2RG	Pathways in cancer	-2,875492074	5,10E-32	1,673303742	1,519132122	1,702369603	0,179241505	0,28321883	0,171058627
FN1	Pathways in cancer	-2,68895037	3,29E-161	6,442144829	5,357421837	6,39023966	0,933491402	0,806792358	0,838133273
EPAS1	Pathways in cancer	-2,640478086	1,22E-154	7,341304357	7,679865696	7,294618335	1,177195146	0,986766712	1,110704485
ITGA6	Pathways in cancer	-2,617343249	7,60E-47	0,93882132	0,885746412	0,859118239	0,147541691	0,164510655	0,096350269
PLCB4	Pathways in cancer	-2,59203244	3,04E-23	0,294883556	0,387842289	0,444020246	0,068606193	0,046071865	0,055653008
TCF7	Pathways in cancer	-2,591096166	3,59E-26	0,61290543	0,55179778	0,505155895	0,084963233	0,055327308	0,100249832
FGFR3	Pathways in cancer	-2,550576886	9,25E-32	0,650676866	0,735125765	0,603322949	0,094754767	0,130526569	0,098544365
GNG2	Pathways in cancer	-2,513274929	8,40E-52	1,453182055	1,469211079	1,420580338	0,274698418	0,186334571	0,220583167
FGFR1	Pathways in cancer	-2,326322276	1,26E-38	1,007924584	1,136890715	1,520907548	0,233511947	0,183809904	0,249789562
GSTM3	Pathways in cancer	-2,260655214	3,07E-38	1,243929217	1,491641487	1,625974362	0,23906191	0,371961187	0,262806622
F2R	Pathways in cancer	-2,227794826	1,28E-11	0,589499199	0,463827055	0,425131445	0,152824346	0,053214415	0,064280929
HMOX1	Pathways in cancer	-2,206109861	1,10E-06	0,322873955	0,696173346	0,706860831	0,213617678	0,054648765	0,066013568
GNG12	Pathways in cancer	-2,202338942	5,82E-57	2,110415918	1,792643665	1,791884144	0,38151205	0,381016795	0,361060831
DLL1	Pathways in cancer	-2,194239888	2,16E-40	1,725449144	1,836352304	1,507999085	0,356705566	0,297513822	0,354099972
CSF1R	Pathways in cancer	-2,084433348	2,37E-58	3,589885545	3,065994133	3,616285705	0,784165199	0,76334352	0,669819425
FZD3	Pathways in cancer	-2,004189619	2,18E-31	0,381666663	0,387349124	0,302101509	0,08211893	0,081931528	0,081206218

MITF	Pathways in cancer	-1,94648696	1,93E-31	1,368704808	1,057801148	1,144355259	0,329050833	0,213842995	0,27840505
HGF	Pathways in cancer	-1,882377412	1,46E-53	5,512371859	4,73250081	5,015520605	1,38558005	1,176402694	1,212791294
LPAR1	Pathways in cancer	-1,731847146	1,91E-09	0,405121203	0,570082141	0,615628849	0,12252962	0,237708329	0,115961335
PTCH1	Pathways in cancer	-1,694956338	1,07E-07	0,156880361	0,228744823	0,124892624	0,035946016	0,064371254	0,052486619
GSTM2	Pathways in cancer	-1,633159807	1,10E-26	2,194158918	2,607881115	2,522619121	0,753393226	0,645873664	0,780190093
GNG7	Pathways in cancer	-1,612850209	9,27E-32	1,692692942	2,250218927	1,985236791	0,624710604	0,53207253	0,642722779
GSTT1	Pathways in cancer	-1,533752554	1,18E-38	9,396115586	8,998919937	9,790337305	2,919915515	3,204818196	2,867086806
PTGS2	Pathways in cancer	-1,526094871	1,93E-11	0,48560444	0,427896207	0,382577169	0,147591878	0,109589445	0,140166802
IL15RA	Pathways in cancer	1,511673431	1,35E-42	1,944581772	2,591032938	2,915398951	6,722669923	6,615441905	6,764823279
AGT	Pathways in cancer	1,529595159	2,06E-246	36,05123511	37,38700298	35,10533772	99,15527949	94,69079023	95,10659977
GNG4	Pathways in cancer	1,614371178	3,65E-40	0,77314697	0,647075357	0,740527208	1,957798205	1,952006164	2,048384128
PMAIP1	Pathways in cancer	1,656902691	5,32E-181	12,49614764	12,9898482	13,9156783	35,96522837	40,15442238	38,863613004
WNT10B	Pathways in cancer	1,703174917	1,98E-54	2,302470186	2,04114542	2,093043829	6,315266635	5,917476274	6,741938716
FOS	Pathways in cancer	1,710991908	2,20E-28	44,06937728	57,69178774	50,91687008	105,5426317	182,9634587	172,4067618
COL4A1	Pathways in cancer	1,743331296	3,14E-40	0,370185341	0,341288432	0,31929729	1,130481226	0,979190918	1,018543132
JUN	Pathways in cancer	1,784371902	4,61E-182	12,68747439	11,86913973	10,91260438	34,24118452	39,69345564	38,130037008
BIRC3	Pathways in cancer	1,969599564	6,02E-17	0,046420138	0,078667249	0,105213405	0,320576629	0,293325983	0,268275628
VEGFA	Pathways in cancer	2,116538748	2,51E-302	12,28051258	12,77846922	13,00196463	46,82642311	54,93777605	50,749022802
WNT10A	Pathways in cancer	2,943538864	2,81E-17	0,027019452	0,089943282	0,041755123	0,463084578	0,42683562	0,486137816
CDKN2A	Pathways in cancer	3,876975738	9,98E-308	5,898315164	4,560515532	3,467872125	60,51595259	59,65604397	61,3875358
CCNA1	Pathways in cancer	4,082678093	2,98E-100	0,223010247	0,236206787	0,344633941	4,335057519	4,617607017	3,708459892
AR	Pathways in cancer	4,332244652	3,20E-134	0,053288502	0,043003297	0,051850375	0,8700304	0,820437407	0,958774295
HLA-A	HLA	1,500948063	4,86E-29	14,54905664	18,58028755	14,15299304	47,35210804	30,59542168	45,453758331
HLA-B	HLA	1,661902278	9,20E-84	42,46103157	34,45779917	31,47552833	106,0238205	106,7504417	103,3461241
HLA-C	HLA	1,761752542	1,72E-45	19,84412887	12,26175654	15,93441671	47,64374672	53,44147907	48,992513661
HLA-H	HLA	2,199677426	4,89E-51	0,191619372	0,182018221	0,175480498	0,751276505	0,860074381	0,70665072
HLA-F	HLA	3,078794235	2,70E-17	0,022534	0,057963783	0,026117571	0,217242403	0,233927996	0,469935938
HOXB-AS3	HOX	-8,726126463	9,98E-308	34,72152666	34,1630436	35,67815556	0,080182273	0,061537916	0,074335392
HOXB6	HOX	-8,603181421	4,48E-268	9,036039883	8,945053584	8,796562016	0,028950913	0	0,020875412
HOXB2	HOX	-8,392894083	1,56E-297	12,09719222	13,69795049	11,69964466	0,020192147	0,072319215	0,021839695
HOXB7	HOX	-8,023055739	3,91E-175	5,637294157	6,340504568	5,807813566	0,023680688	0	0,025612878
HOXB8	HOX	-7,743274673	4,00E-287	9,856245517	9,427493952	9,265873267	0,062104975	0,015888012	0,028788144
HOXB4	HOX	-7,50050364	5,11E-293	8,364666798	9,303818696	9,430674151	0,031822745	0,01424685	0,077443365
HOXA-AS3	HOX	-7,334746166	3,75E-45	0,338715539	0,391373338	0,436201449	0,003880497	0	0
HOXB5	HOX	-7,086856331	1,22E-63	1,233383826	2,015540452	2,051259579	0,008881884	0,015905462	0,009606587
HOXB3	HOX	-6,943522402	9,98E-308	10,03894371	11,83531147	11,54863448	0,102819217	0,104071308	0,048351563
HOXA3	HOX	-6,481631685	3,48E-123	1,495358768	1,569879118	1,52157141	0,013959071	0,016665044	0,01509804
HOXA6	HOX	-6,445089585	7,35E-50	2,880502675	2,833029872	2,225725062	0,04033394	0	0,021812463
HOXB-AS1	HOX	-6,427587706	1,35E-37	1,529802724	1,803071956	2,15673679	0,040586976	0	0
HOXB9	HOX	-6,132389064	8,42E-251	4,705887889	5,257669386	5,056364947	0,047922696	0,064364101	0,084228423

HOXA5	HOX	-5,617956521	4,40E-110	3,2918237	4,301136409	3,77043467	0,068326717	0,034959379	0,095016512
MEIS1	HOX	-5,541029076	3,06E-300	10,3488918	10,14017905	9,965682862	0,157620625	0,2549474	0,208977251

Statistically significant differential expressed genes (adjusted p-value<0.05 and absolute log Fold Change (logFC) > 1.5) were identified for each comparison

Supplemental Table 4. OCI-AML3 CD123 KO vs WT heatmap path

Genes	Pathway	log2 Fold Change	P adj	OCI AML3 wt_1	OCI AML3 wt_2	OCI AML3 wt_3	OCI AML3 123 KO_1	OCI AML3 123 KO_2	OCI AML3 123 KO_3
CTNNA2	Pathways in cancer	-6,568137157	7,37E-26	0,296963897	0,245093466	0,285086599	0,007316361	0	0
SMO	Pathways in cancer	-3,922843744	3,03E-107	2,489918058	2,556711149	2,512160407	0,158226827	0,137206013	0,184463849
GSTM3	Pathways in cancer	-3,348538135	1,64E-55	1,243929217	1,491641487	1,625974362	0,176986085	0,144946777	0,107377767
TCF7	Pathways in cancer	-2,567933208	4,40E-20	0,61290543	0,55179778	0,505155895	0,116272138	0,09522371	0,064663967
NOTCH3	Pathways in cancer	-2,422742289	1,76E-10	0,151065887	0,144365548	0,126965717	0,030166504	0,031764271	0,015251726
ADCY1	Pathways in cancer	-2,089291259	1,70E-07	0,124064648	0,087103487	0,066465054	0,02958795	0,017623072	0,015231203
ITGA6	Pathways in cancer	-2,01530875	1,05E-30	0,93882132	0,885746412	0,859118239	0,191570283	0,225530579	0,220345174
TRAF5	Pathways in cancer	-1,978513009	9,25E-12	0,482958765	0,504465704	0,433365258	0,160441275	0,069156331	0,125517371

VEGFC	Pathways in cancer	-1,945720985	3,62E-30	3,164017925	3,737035931	3,59202658	0,649352419	1,077239792	0,91924758
FZD6	Pathways in cancer	-1,767867168	2,89E-08	0,391586261	0,597449338	0,479074476	0,168028887	0,072426882	0,18779051
GNG12	Pathways in cancer	-1,667226542	4,06E-30	2,110415918	1,792643665	1,791884144	0,591664429	0,587929199	0,547220438
FZD3	Pathways in cancer	-1,606261767	9,95E-17	0,381666663	0,387349124	0,302101509	0,090821155	0,130165086	0,117855673
HGF	Pathways in cancer	-1,593889481	1,57E-36	5,512371859	4,73250081	5,015520605	1,623808571	1,875095459	1,407968552
JUP	Pathways in cancer	-1,565347358	3,88E-07	0,621955744	0,642152333	0,433461342	0,138810637	0,267965011	0,147379148
F2R	Pathways in cancer	-1,56410435	3,11E-07	0,589499199	0,463827055	0,425131445	0,118678671	0,231771726	0,122773591
WNT3	Pathways in cancer	-1,517338271	1,09E-14	1,740560078	1,811721647	1,950854098	0,425055488	0,832065063	0,601724452
WNT7B	Pathways in cancer	1,516567926	6,28E-53	2,772222021	2,874215837	2,906777038	7,806384991	8,089821681	7,99876683
PTGER4	Pathways in cancer	1,532311562	6,65E-130	21,09609365	19,49347581	21,55035752	63,35289141	56,02035718	55,36467735
CXCL8	Pathways in cancer	1,669349021	2,74E-82	88,93638829	88,45301958	93,60412815	323,95181	240,3808031	275,4333319
LAMB2	Pathways in cancer	1,679115255	2,32E-08	0,110487601	0,130400021	0,091063743	0,25152258	0,446311956	0,356064774
PTGER2	Pathways in cancer	1,854723408	1,21E-21	0,517927349	0,548575488	0,440214925	2,021228838	1,712808077	1,649237186
BIRC3	Pathways in cancer	2,239734946	9,27E-20	0,046420138	0,078667249	0,105213405	0,377408633	0,391510678	0,359744346
FOS	Pathways in cancer	2,576679952	1,91E-184	44,06937728	57,69178774	50,91687008	302,5613165	266,2033975	321,3176986
MMP9	Pathways in cancer	2,621082605	2,47E-83	2,499819804	2,277809421	2,122611657	14,04084193	15,19388867	11,77217385
JUN	Pathways in cancer	2,715097085	9,98E-308	12,68747439	11,86913973	10,91260438	69,52209102	76,28420095	79,9776498
CCNA1	Pathways in cancer	3,40029493	2,16E-68	0,223010247	0,236206787	0,344633941	2,765031393	2,734706295	2,823416446
BIRC7	Pathways in cancer	4,230693892	4,54E-58	0	0,184542719	0,338293819	3,38158135	3,539863862	4,229198772
CDKN2A	Pathways in cancer	4,32630044	9,98E-308	5,898315164	4,560515532	3,467872125	92,12705279	88,9794674	83,26501069
IL16	Cytokine-receptor interaction	-1,960658365	6,76E-32	0,684800559	0,745115483	0,673806188	0,200184055	0,174191862	0,159405772
BMPR1B	Cytokine-receptor interaction	-1,926414957	4,82E-26	0,723329458	0,89191508	0,800821669	0,216509631	0,201277035	0,21123589
CSF1	Cytokine-receptor interaction	-1,876411474	2,26E-07	0,195842925	0,323988795	0,329552554	0,035383499	0,115912483	0,075135308
CX3CR1	Cytokine-receptor interaction	-1,630089355	5,76E-42	5,404629241	5,681964	6,146615925	1,769058847	2,064166139	1,608974915
TNFRSF11A	Cytokine-receptor interaction	-1,562372116	3,90E-50	7,153419035	7,005928866	7,355404732	2,127963481	2,573803501	2,374562546
CCR2	Cytokine-receptor interaction	1,606773695	4,32E-91	8,081879508	7,982577606	8,160186196	23,81608879	26,76729489	21,25746618
CXCL8	Cytokine-receptor interaction	1,669349021	2,74E-82	88,93638829	88,45301958	93,60412815	323,95181	240,3808031	275,4333319
CXCL10	Cytokine-receptor interaction	1,720779098	2,44E-14	0,580496039	0,63880172	0,924267041	2,431306139	2,342556967	2,206831912
CXCL2	Cytokine-receptor interaction	1,770294075	5,91E-21	0,960167558	1,33983749	1,621207144	4,279079784	4,049060063	5,136702654
OSM	Cytokine-receptor interaction	2,639390294	6,73E-77	1,038929279	1,268088638	1,070355279	7,114069221	6,456506715	7,480132797
INHBA	Cytokine-receptor interaction	2,853717541	1,09E-48	0,324543992	0,455355488	0,547136092	3,694086109	3,195613896	2,88640489
IL32	Cytokine-receptor interaction	3,30082719	1,76E-52	0,268948862	0,748784849	0,471043052	4,839738988	5,993175753	5,530580052
CCL3	Cytokine-receptor interaction	3,358030574	1,54E-57	1,531724587	1,585769094	1,86875157	21,58580141	13,38388728	15,24790523

TRAF5	IL-17 signaling pathway	-1,978513009	9,25E-12	0,482958765	0,504465704	0,433365258	0,160441275	0,069156331	0,125517371
CXCL8	IL-17 signaling pathway	1,669349021	2,74E-82	88,93638829	88,45301958	93,60412815	323,95181	240,3808031	275,4333319
CXCL10	IL-17 signaling pathway	1,720779098	2,44E-14	0,580496039	0,63880172	0,924267041	2,431306139	2,342556967	2,206831912
CXCL2	IL-17 signaling pathway	1,770294075	5,91E-21	0,960167558	1,33983749	1,621207144	4,279079784	4,049060063	5,136702654
TNFAIP3	IL-17 signaling pathway	2,286425551	9,98E-308	6,85323479	6,934976005	7,018673641	32,32272186	33,68598897	32,90718738
FOS	IL-17 signaling pathway	2,576679952	1,91E-184	44,06937728	57,69178774	50,91687008	302,5613165	266,2033975	321,3176986
MMP9	IL-17 signaling pathway	2,621082605	2,47E-83	2,499819804	2,277809421	2,122611657	14,04084193	15,19388867	11,77217385
JUN	IL-17 signaling pathway	2,715097085	9,98E-308	12,68747439	11,86913973	10,91260438	69,52209102	76,28420095	79,9776498
FOSB	IL-17 signaling pathway	3,523901057	3,52E-130	1,750432586	2,309159946	2,328636902	22,17166973	19,85535404	30,66333062
S100A8	IL-17 signaling pathway	3,613000319	1,97E-179	5,766818985	6,535075952	5,498822337	73,48773892	66,66585677	75,27020648
S100A9	IL-17 signaling pathway	3,731994258	9,98E-308	11,23274012	8,514994435	9,166347002	116,9446108	112,4115545	131,5875766
HLA-E	HLA	-1,617325301	0,000317246	0,320270552	2,058262062	1,985071343	0,462913542	0,51975247	0,402967555
HLA-F	HLA	1,541184738	8,35E-06	0,022534	0,057963783	0,026117571	0,12519192	0,112531575	0,10590356

Statistically significant differential expressed genes (adjusted p-value<0.05 and absolute log Fold Change (logFC) > 1.5) were identified for each comparison

Supplemental Table 5. OCI-AML3 CD33/CD123 KO vs WT heatmap path

Genes	Pathway	log2 Fold Change	P adj	OCI AML3 wt_1	OCI AML3 wt_2	OCI AML3 wt_3	OCI AML3 33/123 KO_1	OCI AML3 33/123 KO_2	OCI AML3 33/123 KO_3
CLDN23	Cell adhesion molecules	-4,942256621	2,92E-49	2,202597489	2,069298686	2,015205188	0,064942522	0,119024888	0
CD226	Cell adhesion molecules	-4,37238523	1,59E-24	0,892092657	0,719910001	0,612718051	0,052216169	0	0,03432815
ITGA6	Cell adhesion molecules	-3,552875452	1,17E-45	0,93882132	0,885746412	0,859118239	0,087275596	0,039989085	0,076502735
CADM1	Cell adhesion molecules	-2,809132297	4,44E-16	0,467336903	0,517089203	0,42128898	0,038466941	0,052875872	0,101156325
ITGB7	Cell adhesion molecules	-2,599345131	1,14E-24	1,432492746	1,429204657	1,510413043	0,338990754	0,22285511	0,077516723
NTNG2	Cell adhesion molecules	-2,343841672	4,88E-08	0,373691871	0,326696137	0,320829559	0,082023813	0,037582754	0,053924405

JAM2	Cell adhesion molecules	-2,180707057	7,17E-11	0,453458148	0,486528899	0,339763312	0,08143542	0,111939467	0,071383441
CLDN7	Cell adhesion molecules	-1,808988888	1,63E-09	0,910452425	0,997580768	1,245265506	0,351443682	0,170501406	0,299002557
OCLN	Cell adhesion molecules	-1,667657886	1,99E-42	3,571572179	3,204111304	3,548910287	1,008847584	0,962769445	1,047666336
NEGR1	Cell adhesion molecules	-1,638626439	9,83E-79	9,961307933	9,51624128	9,662025422	2,77283606	2,971318084	2,999011133
ITGAL	Cell adhesion molecules	1,697801269	1,42E-132	8,327842231	8,253970636	8,66224411	24,76624457	23,70644912	27,94538147
PTK2	Trans misreg in cancer	-8,145788709	2,75E-200	4,617028414	4,802913489	4,700059147	0	0,024875437	0,02379448
CD14	Trans misreg in cancer	-5,757514577	1,84E-47	2,345126855	2,043033629	2,635705425	0,046795055	0,032161764	0,030764181
WT1	Trans misreg in cancer	-5,175999848	2,14E-115	4,376189155	3,885086429	3,870181619	0,114756611	0,105161398	0,08382636
ZEB1	Trans misreg in cancer	-4,945809301	7,93E-59	0,994357278	0,829792336	0,920956757	0,006613857	0,036365093	0,04348107
PBX1	Trans misreg in cancer	-3,541837436	7,12E-58	1,227089411	1,178733998	1,144490394	0,055092483	0,075729003	0,160973813
IGFBP3	Trans misreg in cancer	-3,251425495	4,57E-45	2,097576233	2,635038885	2,726409022	0,20879025	0,242845154	0,295644835
PDGFA	Trans misreg in cancer	-2,955729808	7,40E-35	2,24039097	1,833340455	2,037303892	0,331182956	0,227618668	0,138553894
MITF	Trans misreg in cancer	-2,826381131	1,35E-35	1,368704808	1,057801148	1,144355259	0,124791931	0,114357629	0,227892172
SPINT1	Trans misreg in cancer	-2,787318137	1,13E-31	2,241788594	1,857926527	1,850303923	0,301947924	0,207525729	0,26467699
MEIS1	Trans misreg in cancer	-2,699228694	1,10E-92	10,3488918	10,14017905	9,965682862	1,567494583	1,332959015	1,449697973
ITGB7	Trans misreg in cancer	-2,599345131	1,14E-24	1,432492746	1,429204657	1,510413043	0,338990754	0,22285511	0,077516723
ETV4	Trans misreg in cancer	-2,331744065	5,29E-58	5,275937	4,860168218	5,004515049	0,887665411	0,904606396	1,006159208
CSF1R	Trans misreg in cancer	-2,299353996	1,66E-48	3,589885545	3,065994133	3,616285705	0,693409168	0,577664302	0,649260378
BAIAP3	Trans misreg in cancer	-1,825891225	9,03E-08	0,353699519	0,359338542	0,396933951	0,091499071	0,022867774	0,174992477
MEF2C	Trans misreg in cancer	-1,770338614	8,38E-78	7,469811712	7,38136132	6,886695599	1,994598306	2,056300608	1,89409471
MMP9	Trans misreg in cancer	-1,690288621	6,44E-16	2,499819804	2,277809421	2,122611657	0,723560522	0,397836614	0,8324503
JUP	Trans misreg in cancer	-1,674301302	1,57E-07	0,621955744	0,642152333	0,433461342	0,168638279	0,19869149	0,126704929
RUNX2	Trans misreg in cancer	-1,503269251	2,49E-136	31,70184013	35,05554269	34,60895802	10,87711262	10,93419693	11,64364271
CEBPE	Trans misreg in cancer	1,654935439	3,60E-07	0,290367414	0,539781259	0,470093766	1,857403713	0,976204127	1,185186606
CDKN2C	Trans misreg in cancer	1,942507885	5,59E-198	14,11352025	13,69087683	12,75289296	51,89056038	47,88777619	45,17902528
CCNA1	Trans misreg in cancer	3,932854855	4,36E-71	0,223010247	0,236206787	0,344633941	3,909867091	4,440838237	3,234168088
EFNA2	MAPK signaling pathway	-8,194578983	2,02E-20	0,808880653	0,734353574	0,493835875	0	0	0
RASGRP4	MAPK signaling pathway	-6,481598563	7,80E-88	2,273311569	2,926815587	2,691332625	0	0,036099531	0,051796251
CD14	MAPK signaling pathway	-5,757514577	1,84E-47	2,345126855	2,043033629	2,635705425	0,046795055	0,032161764	0,030764181
VEGFC	MAPK signaling pathway	-4,55989135	3,40E-71	3,164017925	3,737035931	3,59202658	0,18205046	0,083414283	0,132982555
NFATC1	MAPK signaling pathway	-4,102564864	1,19E-141	4,707627254	4,390601548	4,253998427	0,216620488	0,195085516	0,314287355
GNG12	MAPK signaling pathway	-4,066169627	1,16E-65	2,110415918	1,792643665	1,791884144	0,134176249	0,131739954	0,037804567
MAP2K6	MAPK signaling pathway	-4,046429599	9,17E-37	1,751059991	1,880654138	1,750967228	0,158261927	0,093232978	0,029727186
TGFA	MAPK signaling pathway	-3,75156522	3,83E-30	0,774223276	0,66233808	0,682597763	0,068629128	0,0404298	0,025781954
MAP4K1	MAPK signaling pathway	-3,73861965	8,27E-210	17,59459247	20,40021925	20,16048299	1,352430335	1,445906895	1,284284227

FGFR1	MAPK signaling pathway	-3,384218353	1,02E-39	1,007924584	1,136890715	1,520907548	0,154194271	0,064507222	0,096963545
BDNF	MAPK signaling pathway	-3,039356789	1,10E-16	0,282290173	0,389446721	0,256613835	0,021868772	0,03757546	0,050319677
PDGFA	MAPK signaling pathway	-2,955729808	7,40E-35	2,24039097	1,833340455	2,037303892	0,331182956	0,227618668	0,138553894
FGFR3	MAPK signaling pathway	-2,701883092	1,58E-20	0,650676866	0,735125765	0,603322949	0,133299478	0,078527461	0,062595889
CSF1R	MAPK signaling pathway	-2,299353996	1,66E-48	3,589885545	3,065994133	3,616285705	0,693409168	0,577664302	0,649260378
HSPA1A	MAPK signaling pathway	-2,190997161	5,88E-38	0,671036822	0,722737478	0,710387176	0,153088606	0,1530418	0,123517745
TGFB3	MAPK signaling pathway	-2,063666444	1,59E-11	0,50104753	0,567199769	0,64047464	0,122197613	0,167970346	0,096402738
MAP3K12	MAPK signaling pathway	-1,996876872	1,19E-41	3,067524323	3,163683068	3,033173183	0,742961485	0,67020168	0,747924578
IL1B	MAPK signaling pathway	-1,927283377	6,16E-42	14,95043276	18,9917713	18,97748961	4,372276264	4,575386634	4,1169375
TNF	MAPK signaling pathway	-1,781056567	4,54E-09	0,137780351	0,129553162	0,141947993	0,032402373	0,035631713	0,04260418
MEF2C	MAPK signaling pathway	-1,770338614	8,38E-78	7,469811712	7,38136132	6,886695599	1,994598306	2,056300608	1,89409471
MAPK11	MAPK signaling pathway	-1,752693636	2,07E-06	0,659925941	0,663029412	0,503116881	0,191203323	0,047786216	0,251403219
HSPA2	MAPK signaling pathway	-1,743313008	3,93E-22	2,085737762	2,279292522	2,292083302	0,518852211	0,671250509	0,702276599
IL1R1	MAPK signaling pathway	-1,563263732	3,51E-07	0,277902008	0,321770356	0,392117633	0,111388266	0,087492594	0,115074605
HGF	MAPK signaling pathway	-1,523514684	2,55E-34	5,512371859	4,73250081	5,015520605	1,647231806	1,721915613	1,556305644
JUN	MAPK signaling pathway	1,680148167	3,30E-153	12,68747439	11,86913973	10,91260438	36,26660401	33,54302599	35,68019197
DUSP2	MAPK signaling pathway	1,773449529	3,70E-40	3,69412834	3,445965646	2,86421144	10,98403519	9,893263964	10,74931534
PDGFD	MAPK signaling pathway	1,817164091	6,47E-44	2,973120892	2,504653075	2,458721073	9,143282591	9,338848349	7,360705979
FOS	MAPK signaling pathway	2,060637616	1,85E-121	44,06937728	57,69178774	50,91687008	220,2673804	186,9835771	189,2339293
DUSP1	MAPK signaling pathway	2,218056378	3,16E-41	1,83889798	2,331500033	1,453555514	9,081685522	7,404006698	8,344996982
CACNA2D3	MAPK signaling pathway	2,408346315	6,76E-91	1,763616612	2,050284095	1,789978677	9,520520747	9,246047663	9,32805137
EFNA2	PI3K-Akt signaling pathway	-8,194578983	2,02E-20	0,808880653	0,734353574	0,493835875	0	0	0
PTK2	PI3K-Akt signaling pathway	-8,145788709	2,75E-200	4,617028414	4,802913489	4,700059147	0	0,024875437	0,02379448
JAK3	PI3K-Akt signaling pathway	-7,795454423	2,18E-70	0,980163687	0,925592422	0,942896858	0	0	0,010224533
F2R	PI3K-Akt signaling pathway	-6,310017584	7,60E-25	0,589499199	0,463827055	0,425131445	0	0	0,014582706
PRL	PI3K-Akt signaling pathway	-6,173868612	1,09E-24	1,234909662	1,107783161	1,13594979	0	0,039920375	0
ITGB5	PI3K-Akt signaling pathway	-5,673808364	2,37E-105	2,725078292	2,407494921	2,716942921	0,038589894	0,039783661	0,063424785

THBS1	PI3K-Akt signaling pathway	-4,815271876	2,50E-26	0,60957097	0,44943397	0,37109655	0,014596178	0	0,028787623
GNG11	PI3K-Akt signaling pathway	-4,732657663	1,69E-104	16,68182099	15,04304394	14,13721663	0,93016208	0,243539394	0,291195553
VEGFC	PI3K-Akt signaling pathway	-4,55989135	3,40E-71	3,164017925	3,737035931	3,59202658	0,18205046	0,083414283	0,132982555
GNG12	PI3K-Akt signaling pathway	-4,066169627	1,16E-65	2,110415918	1,792643665	1,791884144	0,134176249	0,131739954	0,037804567
GHR	PI3K-Akt signaling pathway	-3,991055432	4,57E-18	0,25070955	0,259222681	0,231387591	0,006878713	0,028366016	0,009044459
COL6A2	PI3K-Akt signaling pathway	-3,853055098	6,04E-103	4,019936893	4,906326762	4,309022249	0,262761453	0,254168302	0,345491251
IRS1	PI3K-Akt signaling pathway	-3,828149039	4,40E-132	2,622380708	2,647517238	2,569267204	0,159620632	0,212762438	0,146277766
TGFA	PI3K-Akt signaling pathway	-3,75156522	3,83E-30	0,774223276	0,66233808	0,682597763	0,068629128	0,0404298	0,025781954
ITGA6	PI3K-Akt signaling pathway	-3,552875452	1,17E-45	0,93882132	0,885746412	0,859118239	0,087275596	0,039989085	0,076502735
LPAR1	PI3K-Akt signaling pathway	-3,527397337	1,41E-16	0,405121203	0,570082141	0,615628849	0,040015089	0,018334642	0,070151656
FGFR1	PI3K-Akt signaling pathway	-3,384218353	1,02E-39	1,007924584	1,136890715	1,520907548	0,154194271	0,064507222	0,096963545
BDNF	PI3K-Akt signaling pathway	-3,039356789	1,10E-16	0,282290173	0,389446721	0,256613835	0,021868772	0,03757546	0,050319677
PDGFA	PI3K-Akt signaling pathway	-2,955729808	7,40E-35	2,24039097	1,833340455	2,037303892	0,331182956	0,227618668	0,138553894
LAMA5	PI3K-Akt signaling pathway	-2,748570664	2,12E-30	0,376123725	0,372048494	0,352799313	0,048055914	0,040650264	0,0631862
FGFR3	PI3K-Akt signaling pathway	-2,701883092	1,58E-20	0,650676866	0,735125765	0,603322949	0,133299478	0,078527461	0,062595889
ITGB7	PI3K-Akt signaling pathway	-2,599345131	1,14E-24	1,432492746	1,429204657	1,510413043	0,338990754	0,22285511	0,077516723
CSF1R	PI3K-Akt signaling pathway	-2,299353996	1,66E-48	3,589885545	3,065994133	3,616285705	0,693409168	0,577664302	0,649260378
COL9A2	PI3K-Akt signaling pathway	-2,204279817	2,21E-13	0,884025694	0,857451973	0,68891282	0,164187665	0,184654649	0,137379294
FN1	PI3K-Akt signaling pathway	-2,010189838	2,31E-71	6,442144829	5,357421837	6,39023966	1,553700098	1,384959014	1,250489417
COL6A1	PI3K-Akt signaling pathway	-1,768481163	6,96E-27	2,506094142	2,256807099	2,456716593	0,670094109	0,797368152	0,499712245
IL7R	PI3K-Akt signaling pathway	-1,57824713	5,23E-06	0,292955471	0,333510046	0,467097615	0,110232873	0,164150846	0,072469711
HGF	PI3K-Akt signaling pathway	-1,523514684	2,55E-34	5,512371859	4,73250081	5,015520605	1,647231806	1,721915613	1,556305644
PDGFD	PI3K-Akt signaling pathway	1,817164091	6,47E-44	2,973120892	2,504653075	2,458721073	9,143282591	9,338848349	7,360705979
TNN	PI3K-Akt signaling pathway	2,332773888	2,97E-67	0,743196788	0,818196836	0,752476005	3,552266057	3,491079836	3,949560641
GNG4	PI3K-Akt signaling pathway	2,514228953	3,32E-81	0,77314697	0,647075357	0,740527208	3,762623684	3,859883921	3,681694135
DDIT4	PI3K-Akt signaling pathway	3,539350609	1,28E-28	12,67307915	13,28999268	13,15075845	80,29109924	96,01123606	247,1663864
BMPR1B	Cytokine-receptor interaction	-9,950531844	6,76E-65	0,723329458	0,89191508	0,800821669	0	0	0

PRL	Cytokine-receptor interaction	-6,173868612	1,09E-24	1,234909662	1,107783161	1,13594979	0	0,039920375	0
LIFR	Cytokine-receptor interaction	-6,073612066	6,01E-34	0,314594936	0,229607555	0,276447571	0,004061899	0,005583403	0
CCL2	Cytokine-receptor interaction	-4,425271319	1,08E-67	9,363668856	9,670791019	11,10721668	0,395972612	0,233269661	0,669398934
GHR	Cytokine-receptor interaction	-3,991055432	4,57E-18	0,25070955	0,259222681	0,231387591	0,006878713	0,028366016	0,009044459
CX3CR1	Cytokine-receptor interaction	-2,944050992	6,67E-90	5,404629241	5,681964	6,146615925	0,658624081	0,667086167	0,774833384
CCL23	Cytokine-receptor interaction	-2,701964522	1,38E-12	4,510435677	2,729907925	2,904293352	0,540011942	0,463930875	0,355016687
TNFRSF11A	Cytokine-receptor interaction	-2,634268645	4,07E-82	7,153419035	7,005928866	7,355404732	1,26961005	1,062283525	0,870961904
CSF1R	Cytokine-receptor interaction	-2,299353996	1,66E-48	3,589885545	3,065994133	3,616285705	0,693409168	0,577664302	0,649260378
TNFRSF10C	Cytokine-receptor interaction	-2,216010592	2,11E-28	4,080497896	4,926384135	5,796993565	0,989931531	0,933078644	1,07847606
TSLP	Cytokine-receptor interaction	-2,139863395	3,56E-17	0,677228877	0,947296209	1,01556149	0,23783828	0,136219854	0,182420629
TGFB3	Cytokine-receptor interaction	-2,063666444	1,59E-11	0,50104753	0,567199769	0,64047464	0,122197613	0,167970346	0,096402738
IL16	Cytokine-receptor interaction	-1,959856353	5,85E-25	0,684800559	0,745115483	0,673806188	0,1722664	0,146255043	0,186532748
IL1B	Cytokine-receptor interaction	-1,927283377	6,16E-42	14,95043276	18,9917713	18,97748961	4,372276264	4,575386634	4,1169375
TNF	Cytokine-receptor interaction	-1,781056567	4,54E-09	0,137780351	0,129553162	0,141947993	0,032402373	0,035631713	0,04260418
LIF	Cytokine-receptor interaction	-1,75974402	1,29E-16	0,970086145	0,978562474	1,041072653	0,266162349	0,336592428	0,223976262
IL18	Cytokine-receptor interaction	-1,659660846	1,82E-11	2,349773615	2,895158554	2,420850624	0,921009906	0,607680686	0,726592565
IL7R	Cytokine-receptor interaction	-1,57824713	5,23E-06	0,292955471	0,333510046	0,467097615	0,110232873	0,164150846	0,072469711
IL1R1	Cytokine-receptor interaction	-1,563263732	3,51E-07	0,277902008	0,321770356	0,392117633	0,111388266	0,087492594	0,115074605
GDF15	Cytokine-receptor interaction	-1,51497259	5,05E-07	1,871659956	1,796310437	1,322245555	0,56341246	0,435631092	0,601901208
CCR2	Cytokine-receptor interaction	1,724663381	1,16E-112	8,081879508	7,982577606	8,160186196	27,3052869	25,67640392	21,64377423
BMP8B	Cytokine-receptor interaction	1,900554517	4,06E-261	46,97610661	47,37799176	46,24179724	163,0767723	157,7031506	169,3162369
SMO	Pathways in cancer	-8,674170302	7,25E-115	2,489918058	2,556711149	2,512160407	0,011307448	0	0
PTK2	Pathways in cancer	-8,145788709	2,75E-200	4,617028414	4,802913489	4,700059147	0	0,024875437	0,02379448
JAK3	Pathways in cancer	-7,795454423	2,18E-70	0,980163687	0,925592422	0,942896858	0	0	0,010224533
RASGRP4	Pathways in cancer	-6,481598563	7,80E-88	2,273311569	2,926815587	2,691332625	0	0,036099531	0,051796251
FZD6	Pathways in cancer	-6,429723103	8,29E-26	0,391586261	0,597449338	0,479074476	0	0	0,014126649
F2R	Pathways in cancer	-6,310017584	7,60E-25	0,589499199	0,463827055	0,425131445	0	0	0,014582706
GSTT1	Pathways in cancer	-6,23290274	4,43E-113	9,396115586	8,998919937	9,790337305	0,246082813	0	0,046223054
ADCY1	Pathways in cancer	-5,643824882	9,01E-15	0,124064648	0,087103487	0,066465054	0	0,004491853	0
CTNNA2	Pathways in cancer	-4,965719442	1,91E-17	0,296963897	0,245093466	0,285086599	0,017777002	0	0

NOTCH3	Pathways in cancer	-4,778760458	1,36E-15	0,151065887	0,144365548	0,126965717	0,005235527	0,007196648	0
GNG11	Pathways in cancer	-4,732657663	1,69E-104	16,68182099	15,04304394	14,13721663	0,93016208	0,243539394	0,291195553
VEGFC	Pathways in cancer	-4,55989135	3,40E-71	3,164017925	3,737035931	3,59202658	0,18205046	0,083414283	0,132982555
PTCH1	Pathways in cancer	-4,342633885	3,54E-15	0,156880361	0,228744823	0,124892624	0,009391251	0,006454511	0,006174032
GNG12	Pathways in cancer	-4,066169627	1,16E-65	2,110415918	1,792643665	1,791884144	0,134176249	0,131739954	0,037804567
PLCB4	Pathways in cancer	-3,856415425	8,67E-22	0,294883556	0,387842289	0,444020246	0,022405055	0,030797532	0,019639488
TGFA	Pathways in cancer	-3,75156522	3,83E-30	0,774223276	0,66233808	0,682597763	0,068629128	0,0404298	0,025781954
TCF7	Pathways in cancer	-3,618362876	4,08E-21	0,61290543	0,55179778	0,505155895	0	0,027738369	0,106132018
ITGA6	Pathways in cancer	-3,552875452	1,17E-45	0,93882132	0,885746412	0,859118239	0,087275596	0,039989085	0,076502735
LPAR1	Pathways in cancer	-3,527397337	1,41E-16	0,405121203	0,570082141	0,615628849	0,040015089	0,018334642	0,070151656
RB1	Pathways in cancer	-3,451681846	9,98E-308	15,20905815	15,66343959	15,99468245	1,505345528	1,302389685	1,152651097
FGFR1	Pathways in cancer	-3,384218353	1,02E-39	1,007924584	1,136890715	1,520907548	0,154194271	0,064507222	0,096963545
LRP5	Pathways in cancer	-3,30251856	1,61E-180	9,1347755	9,221848077	9,232005907	0,765706266	0,944016564	0,923753021
FZD3	Pathways in cancer	-3,037672715	4,89E-30	0,381666663	0,387349124	0,302101509	0,061298229	0,025277789	0,028209239
PDGFA	Pathways in cancer	-2,955729808	7,40E-35	2,24039097	1,833340455	2,037303892	0,331182956	0,227618668	0,138553894
MITF	Pathways in cancer	-2,826381131	1,35E-35	1,368704808	1,057801148	1,144355259	0,124791931	0,114357629	0,227892172
LAMA5	Pathways in cancer	-2,748570664	2,12E-30	0,376123725	0,372048494	0,352799313	0,048055914	0,040650264	0,0631862
FGFR3	Pathways in cancer	-2,701883092	1,58E-20	0,650676866	0,735125765	0,603322949	0,133299478	0,078527461	0,062595889
TRAF5	Pathways in cancer	-2,636408368	6,15E-14	0,482958765	0,504465704	0,433365258	0,051293924	0,141015163	0,026977476
CSF1R	Pathways in cancer	-2,299353996	1,66E-48	3,589885545	3,065994133	3,616285705	0,693409168	0,577664302	0,649260378
ADCY6	Pathways in cancer	-2,211190057	4,18E-50	4,01429265	4,635995236	4,367674366	0,712887518	0,884530136	1,05346882
FZD4	Pathways in cancer	-2,152532845	1,24E-09	0,225649332	0,265266	0,219062862	0,085723427	0,023566735	0,030056863
DLL1	Pathways in cancer	-2,072200235	1,86E-23	1,725449144	1,836352304	1,507999085	0,34468587	0,350961605	0,436423836
TGFB3	Pathways in cancer	-2,063666444	1,59E-11	0,50104753	0,567199769	0,64047464	0,122197613	0,167970346	0,096402738
EPAS1	Pathways in cancer	-2,031594282	8,25E-66	7,341304357	7,679865696	7,294618335	1,676822797	1,484147738	1,935892386
FN1	Pathways in cancer	-2,010189838	2,31E-71	6,442144829	5,357421837	6,39023966	1,553700098	1,384959014	1,250489417
F2RL3	Pathways in cancer	-1,850367144	9,31E-25	3,924053514	3,626503796	2,917074137	0,866471011	0,914543486	0,915490669
KIF7	Pathways in cancer	-1,839800147	1,13E-25	2,041426894	2,249568707	2,016148883	0,667491725	0,369556872	0,585099902
HMOX1	Pathways in cancer	-1,822318423	5,76E-05	0,322873955	0,696173346	0,706860831	0,212608475	0,146123637	0,104830399
FZD1	Pathways in cancer	-1,809842719	8,03E-59	7,936575813	8,004435198	7,903076881	2,10793972	2,096370311	2,145769823
GSTM3	Pathways in cancer	-1,735081454	6,12E-20	1,243929217	1,491641487	1,625974362	0,378839248	0,422225434	0,44426549
MMP9	Pathways in cancer	-1,690288621	6,44E-16	2,499819804	2,277809421	2,122611657	0,723560522	0,397836614	0,8324503
JUP	Pathways in cancer	-1,674301302	1,57E-07	0,621955744	0,642152333	0,433461342	0,168638279	0,19869149	0,126704929
GSTM2	Pathways in cancer	-1,643932535	4,84E-17	2,194158918	2,607881115	2,522619121	0,837580465	0,748358664	0,605709838
PTGS2	Pathways in cancer	-1,627716476	5,64E-08	0,48560444	0,427896207	0,382577169	0,169287073	0,116349279	0,086561491
IL7R	Pathways in cancer	-1,57824713	5,23E-06	0,292955471	0,333510046	0,467097615	0,110232873	0,164150846	0,072469711
HGF	Pathways in cancer	-1,523514684	2,55E-34	5,512371859	4,73250081	5,015520605	1,647231806	1,721915613	1,556305644
ADCY3	Pathways in cancer	-1,521034946	4,84E-50	10,086965	10,01459745	9,888267203	3,422000153	2,787933284	3,513583028
PTGER2	Pathways in cancer	1,512557525	2,70E-13	0,517927349	0,548575488	0,440214925	1,313037512	1,265756199	1,479809265
JUN	Pathways in cancer	1,680148167	3,30E-153	12,68747439	11,86913973	10,91260438	36,26660401	33,54302599	35,68019197

AGT	Pathways in cancer	1,838006421	4,72E-200	36,05123511	37,38700298	35,10533772	120,8902829	115,0880746	126,51173
FOS	Pathways in cancer	2,060637616	1,85E-121	44,06937728	57,69178774	50,91687008	220,2673804	186,9835771	189,2339293
GNG4	Pathways in cancer	2,514228953	3,32E-81	0,77314697	0,647075357	0,740527208	3,762623684	3,859883921	3,681694135
CCNA1	Pathways in cancer	3,932854855	4,36E-71	0,223010247	0,236206787	0,344633941	3,909867091	4,440838237	3,234168088
CDKN2A	Pathways in cancer	4,804144913	9,98E-308	5,898315164	4,560515532	3,467872125	111,8419825	116,0005795	126,5743829
HOXB5	HOX	-7,161987444	1,13E-37	1,233383826	2,015540452	2,051259579	0	0,03189684	0
HOXB7	HOX	-7,09950834	1,07E-96	5,637294157	6,340504568	5,807813566	0	0	0,122020743
HOXB6	HOX	-6,821399141	2,55E-156	9,036039883	8,945053584	8,796562016	0,075637114	0,034656411	0,099451274
HOXA6	HOX	-6,517840015	9,21E-29	2,880502675	2,833029872	2,225725062	0	0	0,069276947
HOXB2	HOX	-6,382323093	3,96E-156	12,09719222	13,69795049	11,69964466	0,184638915	0,145029078	0,069363435
HOXA-AS3	HOX	-6,156205958	5,89E-24	0,338715539	0,391373338	0,436201449	0	0	0,013330161
HOXB3	HOX	-5,940343065	1,73E-220	10,03894371	11,83531147	11,54863448	0,186869804	0,144487924	0,168922395
HOXB-AS3	HOX	-5,693656059	2,69E-279	34,72152666	34,1630436	35,67815556	0,598525984	0,699313367	0,590227813
HOXB8	HOX	-5,417860658	2,01E-153	9,856245517	9,427493952	9,265873267	0,208614048	0,063723692	0,335250261
HOXB4	HOX	-5,331586694	2,48E-141	8,364666798	9,303818696	9,430674151	0,290990203	0,171423942	0,136645626
HOXB-AS1	HOX	-5,170407136	1,10E-19	1,529802724	1,803071956	2,15673679	0,053018738	0,072878476	0
HOXA5	HOX	-4,724258475	5,06E-59	3,2918237	4,301136409	3,77043467	0,127507346	0,140215198	0,134122176
HOXA3	HOX	-4,703567473	7,60E-60	1,495358768	1,569879118	1,52157141	0,060782414	0,05013016	0,047951765
HOXB9	HOX	-4,219789706	7,47E-106	4,705887889	5,257669386	5,056364947	0,328657268	0,172101172	0,22635601
MEIS1	HOX	-2,699228694	1,10E-92	10,3488918	10,14017905	9,965682862	1,567494583	1,332959015	1,449697973

Statistically significant differential expressed genes (adjusted p-value<0.05 and absolute log Fold Change (logFC) > 1.5) were identified for each comparison

Supplemental Table 6. Summary of the calculated parameters for all the system obtained after 30ns MD simulations.

	WT	N18K	E22R	E43N	F113A	Mut4
RMSD (nm)*	0.15 (0.02)	0.16 (0.02)	0.15 (0.02)	0.17 (0.03)	0.17 (0.03)	0.17 (0.03)
HBond median (n°)	5	4	5	4	4	4
HBond max (n°)	11	9	11	9	10	8
HBond min (n°)	2	1	1	1	1	0
ΔG (KCal/mol)*	-44.31 (0.9)	-31.27 (0.4)	-42.16 (0.7)	-34.41 (0.9)	-35.96 (0.8)	-24.65 (0.5)

*Results are reported as mean and (Standard Error of Mean).

Supplemental Table 7. Results of the HB interactions where a percentage of occupancy is greater than 33% (one third of the 100ns trajectory).

WT			Mut4		
IL-3Rα	**IL3**	**Occupancy**	**IL-3Rα**	**IL3**	**Occupancy**
LYS116	GLU276	95%	LYS116	GLU276	94%
LYS116	ASN233	83%	LYS116	ASN233	86%
LYS28	GLU280	82%	ASN120	ASN233	77%
GLY71	GLU43	80%	ALA72	ASN43	58%
ALA72	GLU43	76%	ARG234	ALA121	51%
ARG277	ASP21	71%	GLY71	ASN43	43%
LYS235	GLU119	50%	LYS28	ARG277	42%
GLN178	THR117	47%	ARG277	ASP21	36%
ARG234	GLU119	46%	ARG255	ASP21	36%
LYS54	GLU43	38%	ARG234	ASN120	35%

Supplemental Table 8. AML patients' characteristics

ID	Subtype	CD33%	CD123%	Karyotype	Prognosis
UPN1	M4	93	99	46, XY, inv(16)(p13q22)(20)	HR
UPN2	M5a	56	97	48, XXY, +21c(22)	HR
UPN3	M5a	73	45	47, XY, +9, t(11;17)(q23;q12 or q21)(20)	HR
PDX	M5a	98	96.5	46,XY,t(10;11)(p12;q23),der(14)t(1;14)(q?21;q11)[20]	HR

Supplemental Figure Legends

Supplemental Figure 1: Gene Ontology (GO)-term enrichment analysis reveals massive gene deregulation in KO clones compared to OCI-AML3 wt.

Bar plots represent up and down different expressed genes (DEGs) identified for each comparison (OCI-AML3 CD33 KO, CD123 KO and CD33/CD123 KO vs OCI-AML3 wt). In y axis per each GO-Terms p-value has been reported in round brackets; x axis represents number of DEGs, with up regulated and down regulated genes distinguished by red and blue color, respectively. Bar plots were generated with the ggplot2 R package.

Supplemental Figure 2: CD33.CCR does not induce CIK cell effector functions *per se.*

(**A)** CD33.CCR and CD33.CAR vector scheme.

(**B)** Flow cytometric analysis of $CD3^+/CD56^+$, $CD3^+/CD4^+$, $CD3^+/CD8^+$ and memory phenotype. Mean ± SEM from 3 independent CAR-CIK donors is shown. Tn=T naïve; Tcm= T central memory; Tem= T effector memory; Temra= Terminally differentiated effector memory.

(**C**) Short-term (E:T ratio of 5:1) cytotoxicity. Mean ± SEM from 3 independent CAR-CIK donors is shown.

(D) Cytokine release against KG-1 cells. Mean ± SEM from 3 independent CAR-CIK donors is shown.

Supplemental Figure 3A: IL3 mutants do not affect conformational stability of CD123 binding.

(A) Time dependence graphical representation of backbone conformation (RMSD) for IL3 in complex with IL3Rα during 30ns molecular dynamics simulation and respect to the first frame.

(**B)** Probability distribution functions of RMSD.

(**C)** Total number of hydrogen bonds between IL3 and IL3Rα during 30ns molecular dynamics simulation.

(D) Probability distribution functions of hydrogen bonds. Wild-type (purple), mutants (red).

Supplemental Figure 3B: IL3 Mut4 shows the lowest free binding energy among mutants.

Box-plot of free binding energy of the last 10ns of trajectories of WT and all mutants. Data are reported as Mean± SEM.

Supplemental Figure 3C. IL3 Mut4 do not affect conformational stability during 100ns MD simulation

(**A)** Time dependence graphical representation of backbone conformation (RMSD), Radius of Gyration and Hydrogen Bonds for IL3 in complex with IL3Rα during 100ns molecular dynamics simulation.

(**B)** Probability distribution functions of RMSD, Radius of Gyration and Hydrogen Bonds.

Supplemental Figure 3D: Th1/Tc1 cytokine release after long-term cytotoxicity assays of KG-1 and TIME cells co-cultured with NT, IL3z wt- and IL3z mut- engineered CIK cells.

Median from 3 independent experiments is shown for each condition.

Supplemental Figure 4: CAR expression profile of IL3z CARs and DC CARs (wild type and mutated variants) before colony assays.

Flow cytometric analysis on CAR CIK cells at the end of the 21-days differentiation process performed as described in Materials and Methods.

Supplementary Figure 5: Low affinity dual CAR CIK cells unveil reduced toxicity against $CD34^+CD38^+$ CMP subpopulation.

Residual quantification of CD34+CD38+ HSPCs after exposure with different CIK conditions was evaluated by staining HSPC within different lineage markers including CD123 and CD45RA (common myeloid progenitors CMP: $CD123^+/CD45RA^-$; granulocyte–monocyte progenitors GMP: $CD123^+/CD45RA^+$; megakaryocyte-erythroid progenitor MEP: $CD123^-/CD45^-$).

Supplementary Figure 6: Low affinity Dual CAR CIK cells preserve anti-leukemic efficacy in vitro.

(A) Flow cytometric analysis of $CD3^+/CD56^+$, $CD3^+/CD4^+$, $CD3^+/CD8^+$ and memory phenotype of DC wt- and DC mut- CIK cells. Mean ± SEM from 4 independent CAR CIK donors is shown. Tn=T naïve; Tcm= T central memory; Tem= T effector memory; Temra= Terminally differentiated effector memory.

(**B)** Expression of IL3 and scFv CD33 on the surface of DC wt- (n=4) and DC mut- CIK cells (n=4) by flow cytometry at the end of the differentiation.

(**C)** Representative dot plots of long-term cytotoxicity of NT and all the single and Dual CAR CIK cells against KG-1 cells. Y axis represents $CD3^+$ CIK cells and X axis KG-1 cells labelled with Ct-PE.

(**D)** Percentage of KG-1 cell survival after 1-week long-term cytotoxicity with NT and all the single and dual CAR CIK cells.

(**E)** CD3 events representing CIK cell proliferation after 1-week long-term cytotoxicity against KG-1 cells. Mean ± SEM from 2 independent CAR CIK donors is shown.

Supplementary Figure 7: Low affinity dual CAR CIK cells improve *in vivo* efficacy in an "AML treatment model".

(A) Schematic of the Luc KG-1 xenograft model. Not-irradiated NSG mice were injected via tail vein on day 0 with 1×10^6 KG-1 cells stably expressing GFP/luciferase. Mice were randomized to 3 treatment groups each receiving tree injection of vehicle or gene-modified CIK cells at day 14, 24 and 34 (n = 4 per group). BLI was measured weekly to quantify AML burden.

(**B)** Tumor burden imaged for 94 days showing suppression of leukemic growth in mice treated with Dual CAR CIK cells.

(**C)** Average BLI for KG-1–engrafted mice with leukemic progression in those untreated or treated with single targeting IL3z mut (blue), and leukemic control in those treated with DC mut (orange) CIK cells.

(**D)** Kaplan–Meier curves of overall survival. P-values indicate comparisons between the KG-1 only cohort and the CAR CIK-treated ones.

Supplementary Figure 8: Dimerization rational for the design of the novel Dual CAR.

A and **B,** IL2 and IFNg production by IL3z mut-, CD33 CAR-, CD33 CCR- and DC mut- redirected CIK cells (former version, with the two chimeric receptors carrying the same spacer/transmembrane domains IgG1-Fc spacer - CD28 transmembrane) following stimulation with wt-, CD123 KO- or CD33KO- KG-1 and CD123-CD33- KG-1.

Supplemental Figure 1

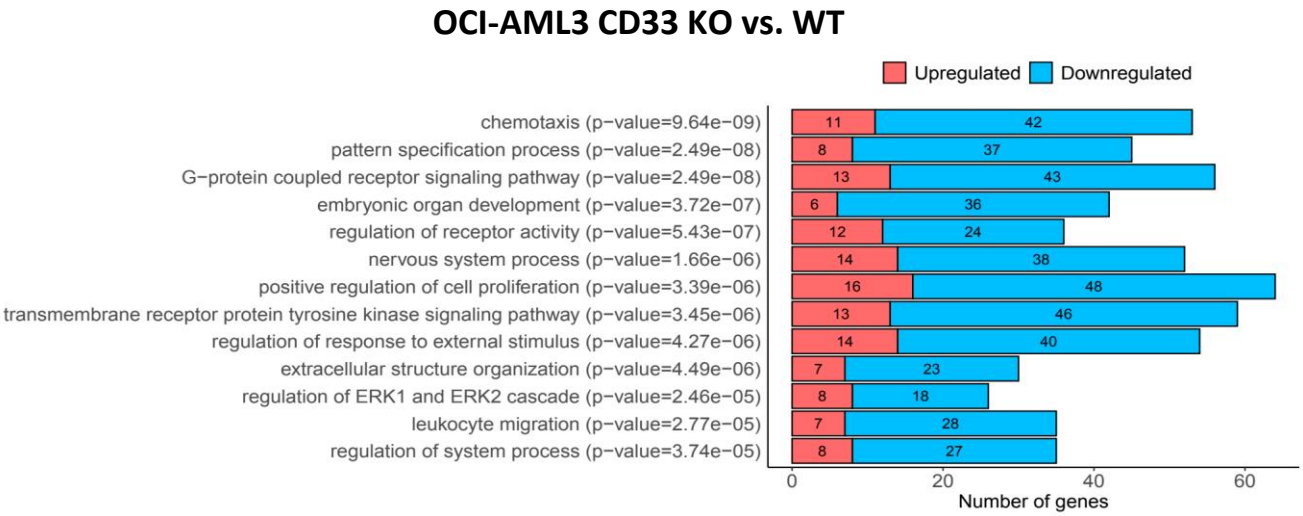

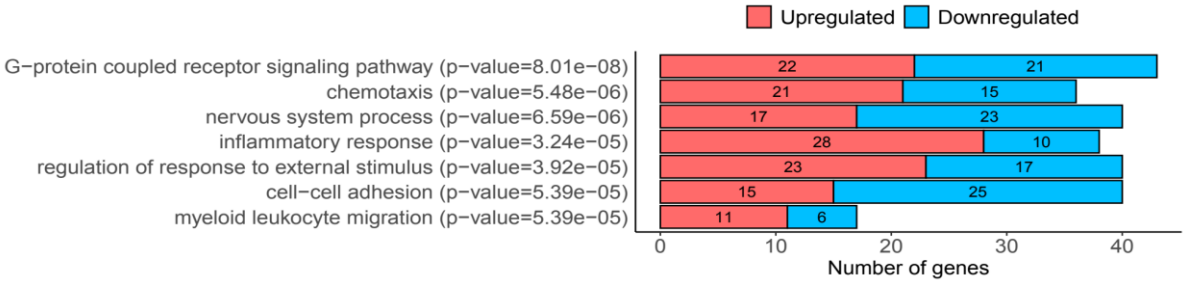

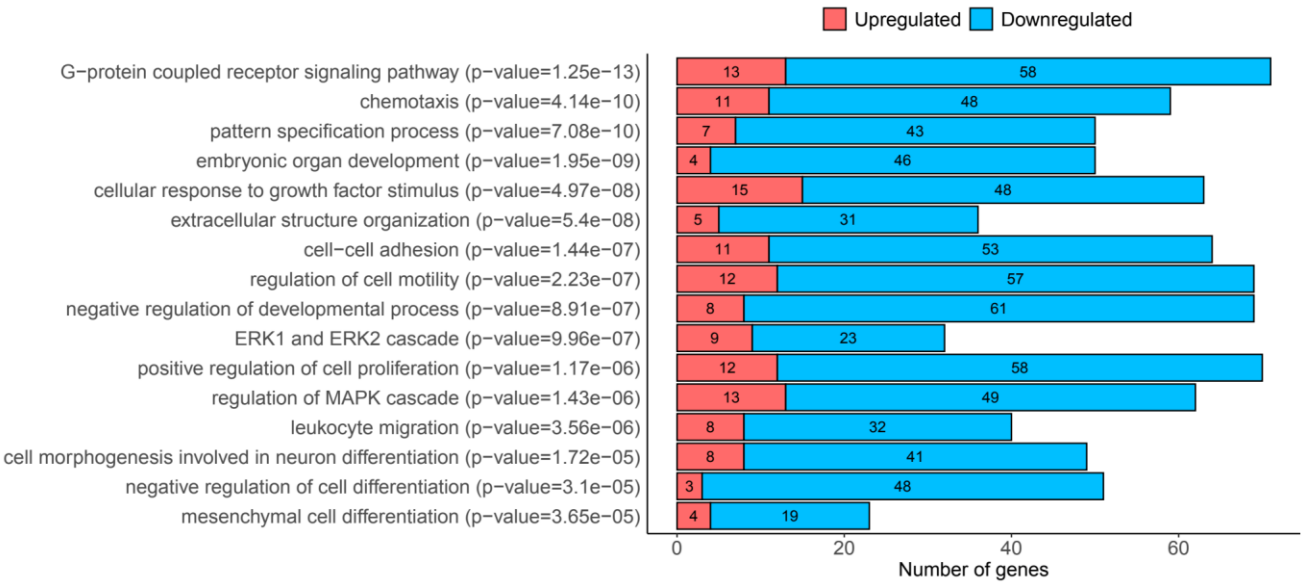

Supplemental Figure 2

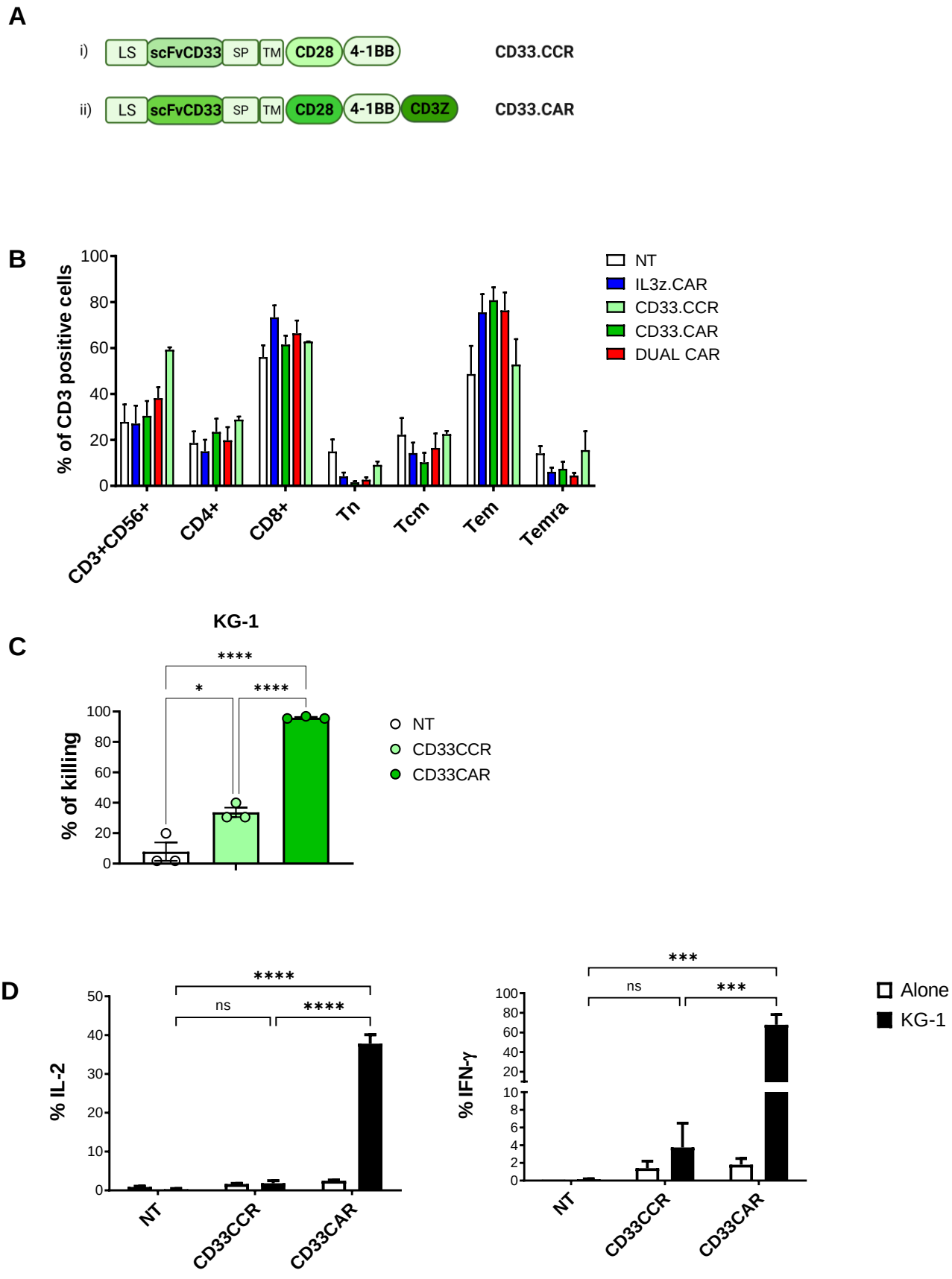

Supplemental Figure 3

Supplemental Figure 3A

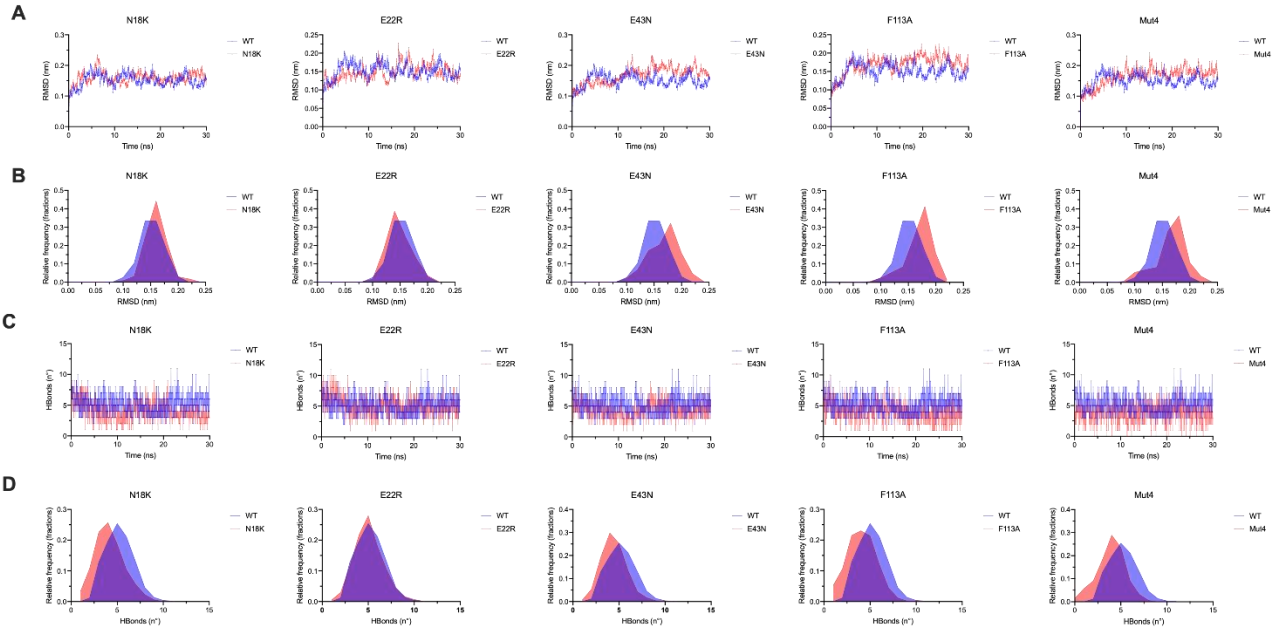

Supplemental Figure 3B

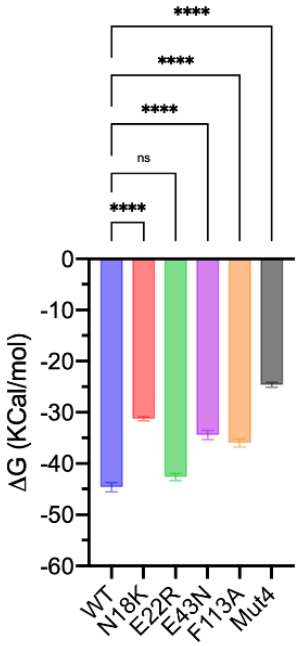

Supplemental Figure 3C

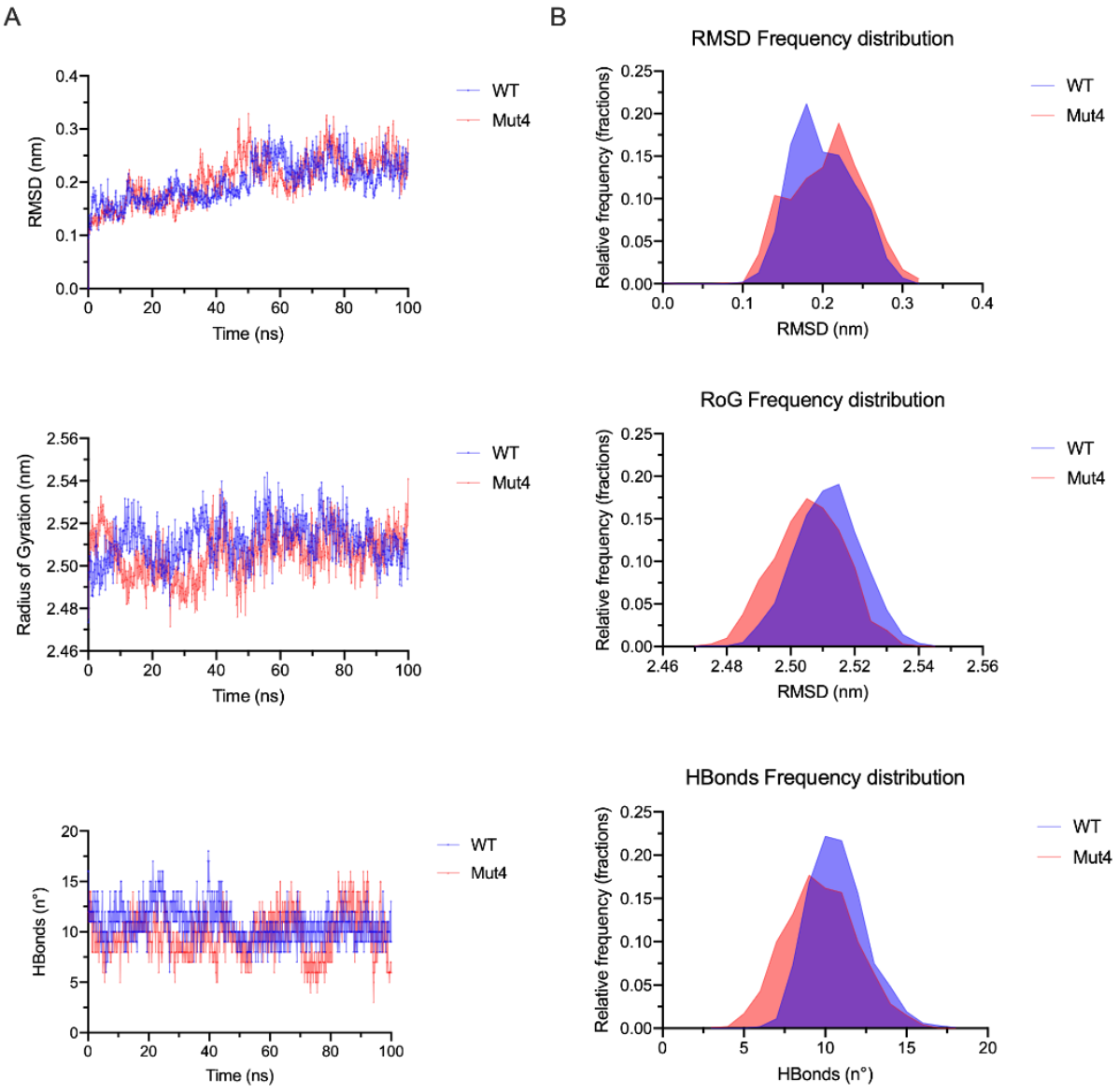

Supplemental Figure 3D

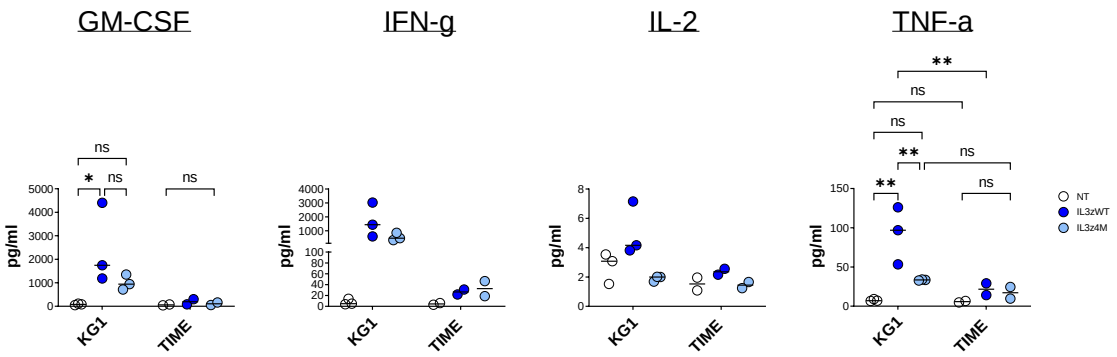

Supplemental Figure 4

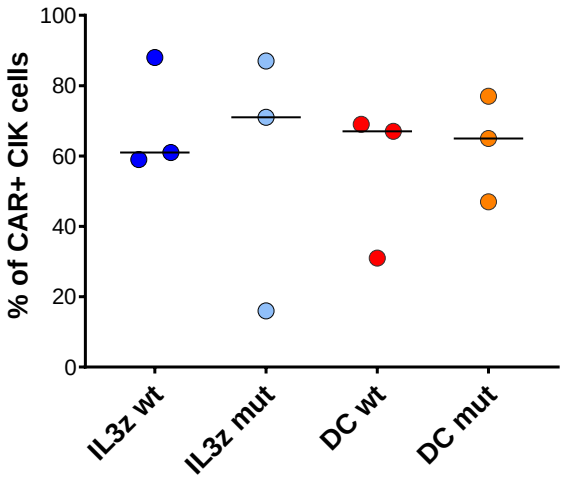

Supplemental Figure 5

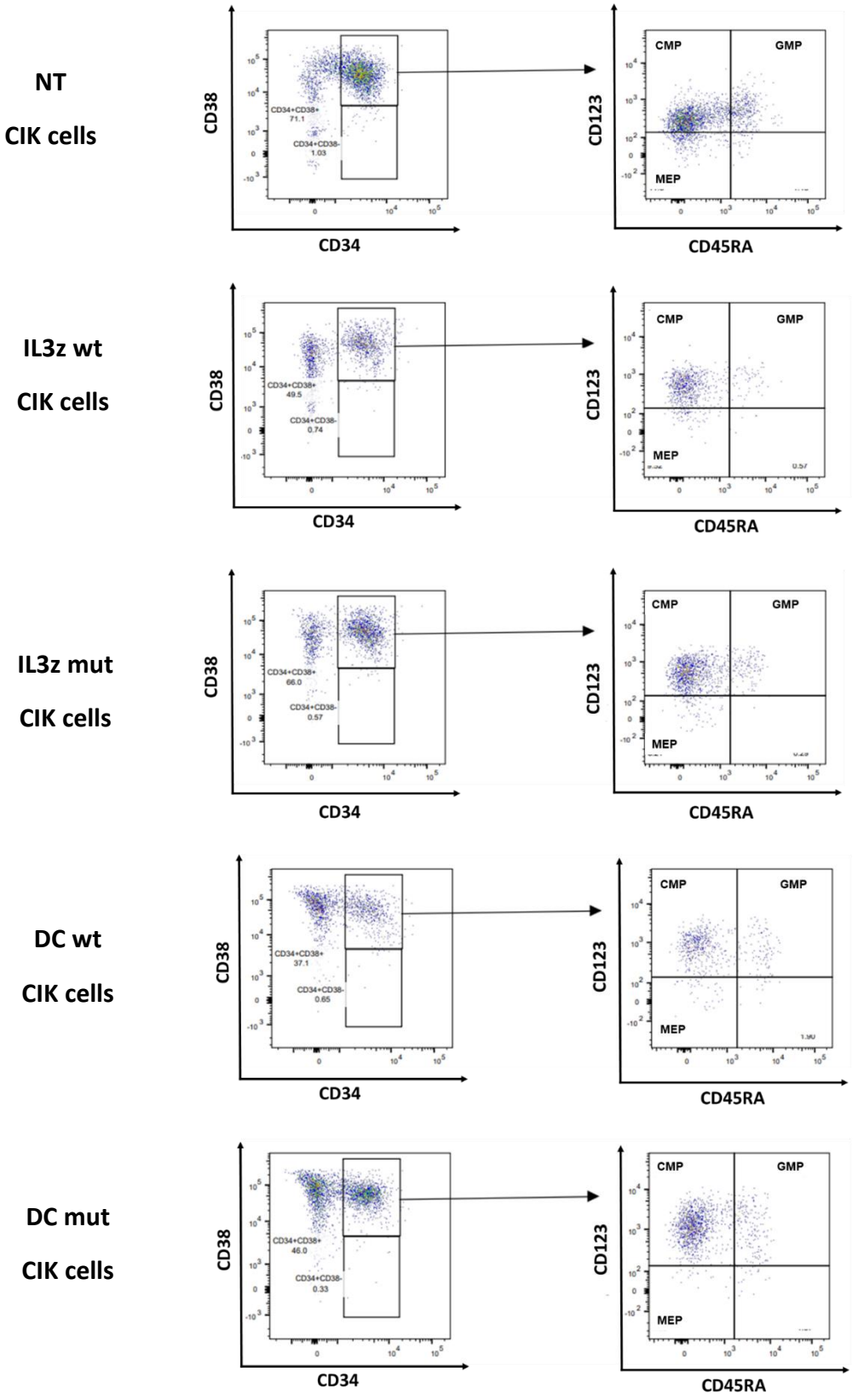

Supplemental Figure 6

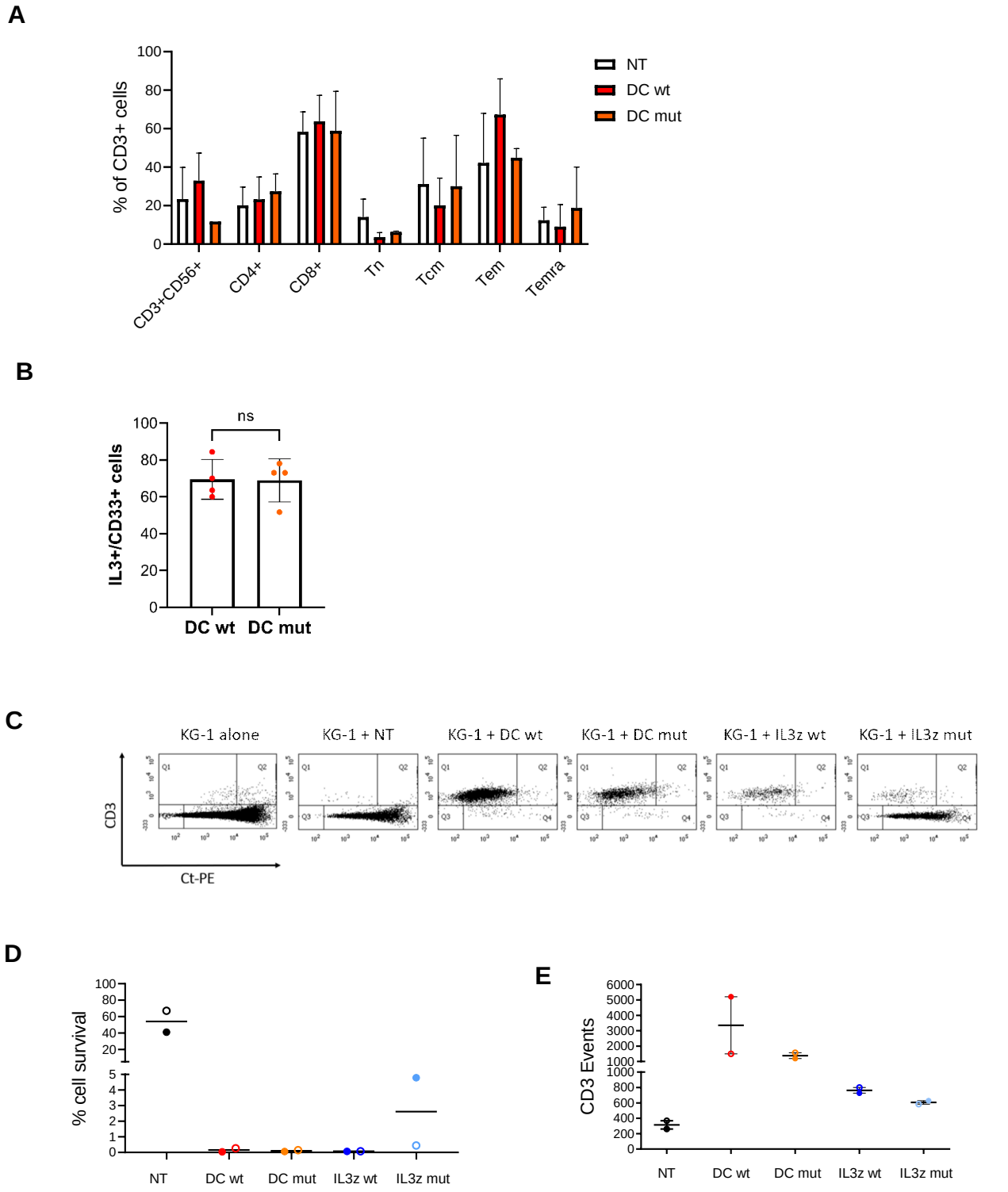

Supplemental Figure 7

A

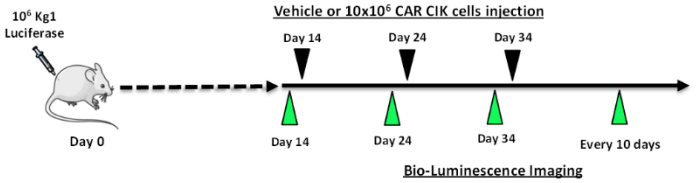

B

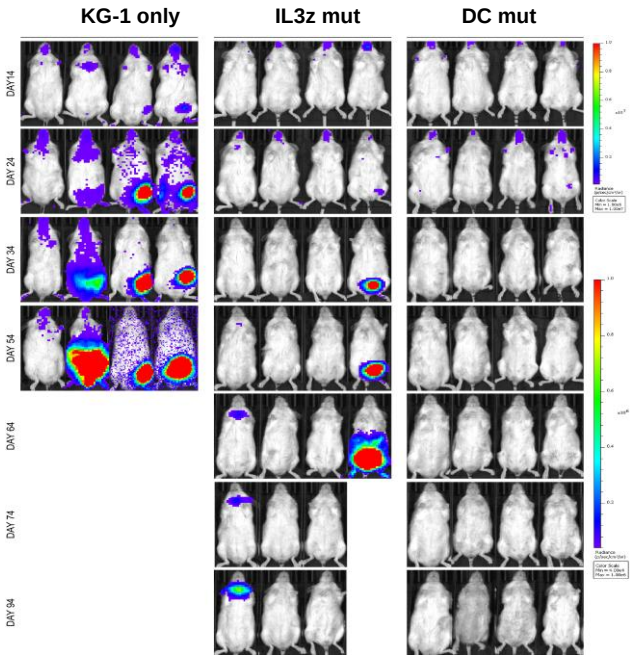

C

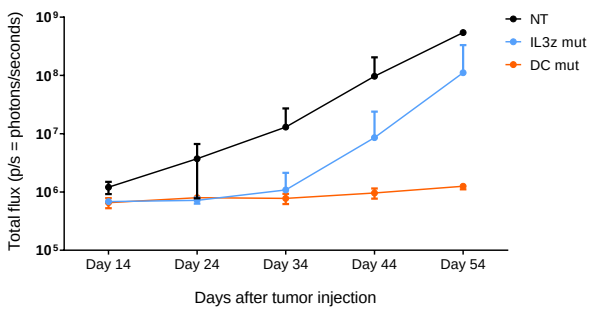

D

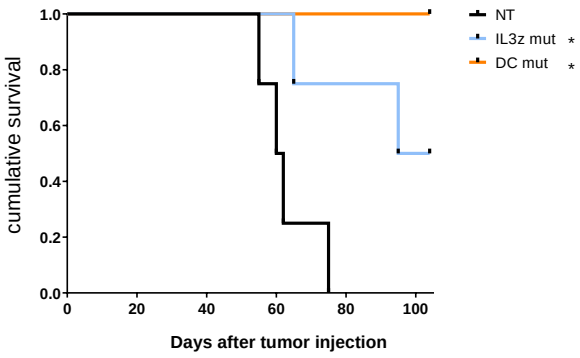

Supplemental Figure 8

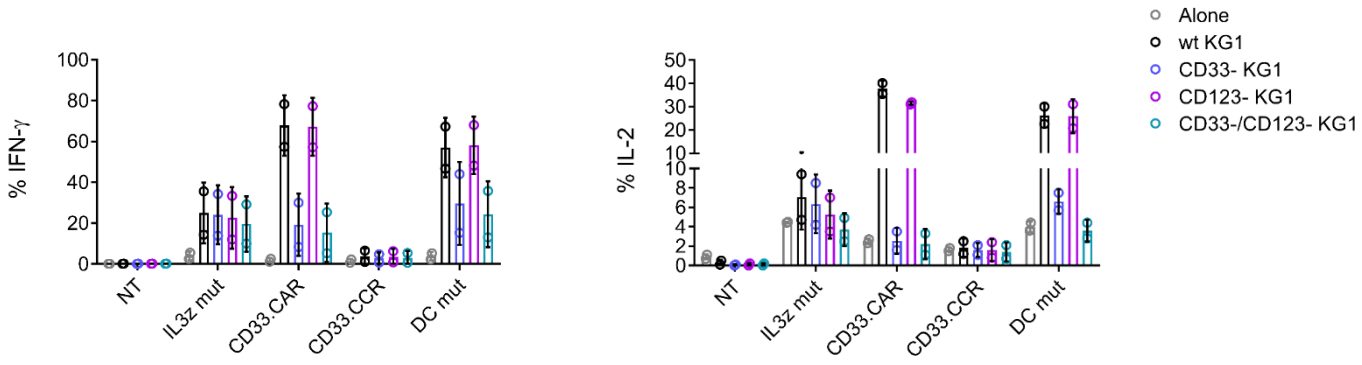

References

1. Pliatsika V, Rigoutsos I. “Off-Spotter”: very fast and exhaustive enumeration of genomic lookalikes for designing CRISPR/Cas guide RNAs. *Biol. Direct*. 2015;10:4.

2. Spinozzi G, Tini V, Adorni A, Falini B, Martelli MP. ARPIR: automatic RNA-Seq pipelines with interactive report. *BMC Bioinformatics*. 2020;21(Suppl 19):574.

3. Tettamanti S, Marin V, Pizzitola I, et al. Targeting of acute myeloid leukaemia by cytokine-induced killer cells redirected with a novel CD123-specific chimeric antigen receptor. *Br. J. Haematol.* 2013;161(3):389–401.

4. Rotiroti MC, Buracchi C, Arcangeli S, et al. Targeting CD33 in Chemoresistant AML Patient-Derived Xenografts by CAR-CIK Cells Modified with an Improved SB Transposon System. *Mol. Ther.* 2020;28(9):1974–1986.

5. Broughton SE, Hercus TR, Nero TL, et al. A dual role for the N-terminal domain of the IL-3 receptor in cell signalling. *Nat. Commun.* 2018;9(1):1–15.

6. Webb B, Sali A. Comparative Protein Structure Modeling Using MODELLER. *Curr. Protoc. Bioinforma.* 2016;54:5.6.1-5.6.37.

7. Schymkowitz J, Borg J, Stricher F, et al. The FoldX web server: an online force field. *Nucleic Acids Res.* 2005;33(Web Server issue):W382-8.

8. Piana S, Robustelli P, Tan D, Chen S, Shaw DE. Development of a Force Field for the Simulation of Single-Chain Proteins and Protein-Protein Complexes. *J. Chem. Theory Comput.* 2020;16(4):2494–2507.

9. Van Der Spoel D, Lindahl E, Hess B, et al. GROMACS: fast, flexible, and free. *J. Comput. Chem.* 2005;26(16):1701–18.

10. Piana S, Donchev AG, Robustelli P, Shaw DE. Water dispersion interactions strongly influence simulated structural properties of disordered protein states. *J. Phys. Chem. B.* 2015;119(16):5113–23.

11. Valdés-Tresanco MS, Valdés-Tresanco ME, Valiente PA, Moreno E. gmx_MMPBSA: A New Tool to Perform End-State Free Energy Calculations with GROMACS. *J. Chem. Theory Comput.* 2021;17(10):6281–6291.